STANAG 1008 Design Constraints for Pulsed Loads in the Frame of the All Electric Ship Concept

George J. Tsekouras[a], Fotis D. Kanellos[b], John M. Prousalidis[c] and Ioannis K. Hatzilau[a]

[a]Hellenic Naval Academy, Department of Electrical Engineering and Computer Science, Terma Hatzikiriaku, 18539, Piraeus, Greece
[b]Hellenic Transmission System Operator,Kastoros 72, Piraeus, 18545, Greece
[c] National Technical University of Athens, School of Naval Architecture and Marine Engineering, 9, Iroon Polytecheniou Street, 157 80, Zografou Campus, Athens, Greece

Abstract. A design issue of ship electric power systems, conventional or All Electric Ship (AES), is to moderate power quality problems caused by the so-called "pulsed loads", i.e loads with periodic high power consumption in short time intervals, causing the relative power supply quality phenomenon referred to as "voltage/frequency modulation". Voltage/frequency modulation may affect the operation of several sensitive electrical ship subsystems.

NATO standard, STANAG 1008, imposes certain design constraints for pulsed loads, so that in a Low Voltage (LV) ship service power supply system the voltage and frequency modulation do not exceed 2% and 0,5%, respectively. These constraints are related with two inequalities involving the power factor of the pulsed load and the ratio between the apparent power of the pulsed load and the full rated apparent power of the supply at the occurrence of the pulse. In a former work of the authors, it was shown that STANAG 1008 guideline for conventional ship electric systems seems to be a method leading to a rough estimation of pulsed loads limits, because it does not take into account certain parameters of the pulsed load and the power grid affecting the entire phenomenon, e.g. the periodicity, the duty cycle of the pulsed load etc.

In this paper, an effort is made to examine and validate the aforementioned STANAG 1008 design constraints in the frame of the All Electric Ship (AES) concept. The voltage and frequency modulation in the LV sub-networks of a AES is studied via simulations in Matlab / Simulink, taking into account various parameters affecting the entire phenomenon such as: pulsed load period, duty cycle and point connection, the technical characteristics of the generators (like subtransient reactance, intertia) and their associated frequency and voltage controllers (like governor and automatic voltage regulator (AVR) gains etc), the service load factor of the generator at the time of the pulsed load occurrence, the equivalent length of the cable between the pulsed load and the generator etc. The respective results are presented and the effects of the respective parameters on the pulsed load limit curve of STANAG 1008 are commented comparing three different cases of power systems: conventional ship, AES with pulse load–connected to low voltage system, AES with pulse load connected to high voltage system. Finally, general conclusions are derived for the effect of the aforementioned parameters on voltage/frequency modulation and on maximum acceptable pulsed load installed power.

Keywords: All Electric Ship (AES), ship electric power system, STANAG 1008, pulsed loads, voltage and frequency modulation, modeling.
PACS: 84.70.+p

INTRODUCTION

Modern ship buildings are characterized by extensive electrification of the equipment installed onboard. This electrification has emerged a series of electric Power Supply Quality (PSQ) problems, which necessitate extent investigation and development-modification of relative standards. One of the most significant issues of Power Supply Quality (P.S.Q.) for continental and ship electric networks is the "Voltage and Frequency Modulation". More specifically, "Modulation" is defined as, [7-9], "voltage and frequency periodic or quasi-periodic variations such as might be caused by regularly or randomly repeated loading with frequency less than nominal". Electric loads causing "modulation" are loads, which require high power for a very short time interval (in the order of a few seconds or even up to some milliseconds) and are known as "*Pulsed Loads*" [4-9]. This operation is often repeated on a regular or almost regular basis introducing a periodicity on the entire phenomenon. Representative examples of pulsed loads are sonars, radars, controlled heaters, electromagnetic aircraft launch systems and electromagnetic guns (such as rail guns, coil guns, lasers, high energy microwaves).

Today, these systems will be among the dominating ones aboard the All Electric Ship (AES), where the most of the installed systems are electrified including propulsion. Pulsed loads of rather small power demand can be directly connected to the electric power grid. On the contrary pulsed loads of larger power demands are interfaced to the network via energy storage devices, pulse forming networks and power electronics, where the power system does not actually interact directly with the pulsed load itself, but with these intermediate systems. Experience from continental and ship power systems indicates that the primary effects of pulse loading are manifested in the areas of voltage flicker, dynamic and transient stability, excitation of torsional frequencies in generators etc [4]. Voltage and frequency modulation may affect the operation of several subsystems of the ship such as radarscopes, communication equipment, missile guidance systems, gear systems etc.

To quantify voltage and frequency modulation, the difference between maximum and minimum value is used as a percentage of the double of the nominal value as shown in (1):

$$M_V = \frac{V_{\max} - V_{\min}}{2V_n} \quad (1)$$

$$M_f = \frac{f_{\max} - f_{\min}}{2f_n} \quad (2)$$

Voltages in (1) may be used in rms, peak or mean values.

In Fig. 1, voltage and frequency modulation provoked by a rectangular pulsed load is shown.

Up to now, few standards, namely IEEE-45, STANAG-1008 (of NATO), and USA-MIL-1399 [7-9] have dealt with this issue to some extent, and have released relevant rules. Especially, in IEEE-45 the respective parameters have not been quantified, while USA-MIL-1399 is overlapped with STANAG-1008. The following analysis will be based on STANAG-1008, which is the NATO naval standard dealing with Power Supply Quality (P.S.Q.) issues.

STANAG 1008 (edition 9) [8] defines voltage and frequency modulation and sets the limits for the low voltage (LV) shipboard electrical power systems (440 V, 115 V, 60 Hz, 400 Hz), which are **2%** and **0.5%,** respectively. STANAG 1008 deals only with the *Ship Service Power Supply System* and explicitly excludes electric propulsion systems. However, up-to-now there is no a NATO standard or other navy standard for the All Electric Ship power system dealing with electric propulsion and high voltage (HV) shipboard electrical power systems (rms line to line voltages > 1000 V). Under these conditions STANAG 1008's rules can be used as a reference,

especially taking into consideration that in AES networks there will be a LV service power system with equipment of more or less similar technology to that of the conventional ships, and therefore, with similar operating constraints concerning voltage and frequency modulation.
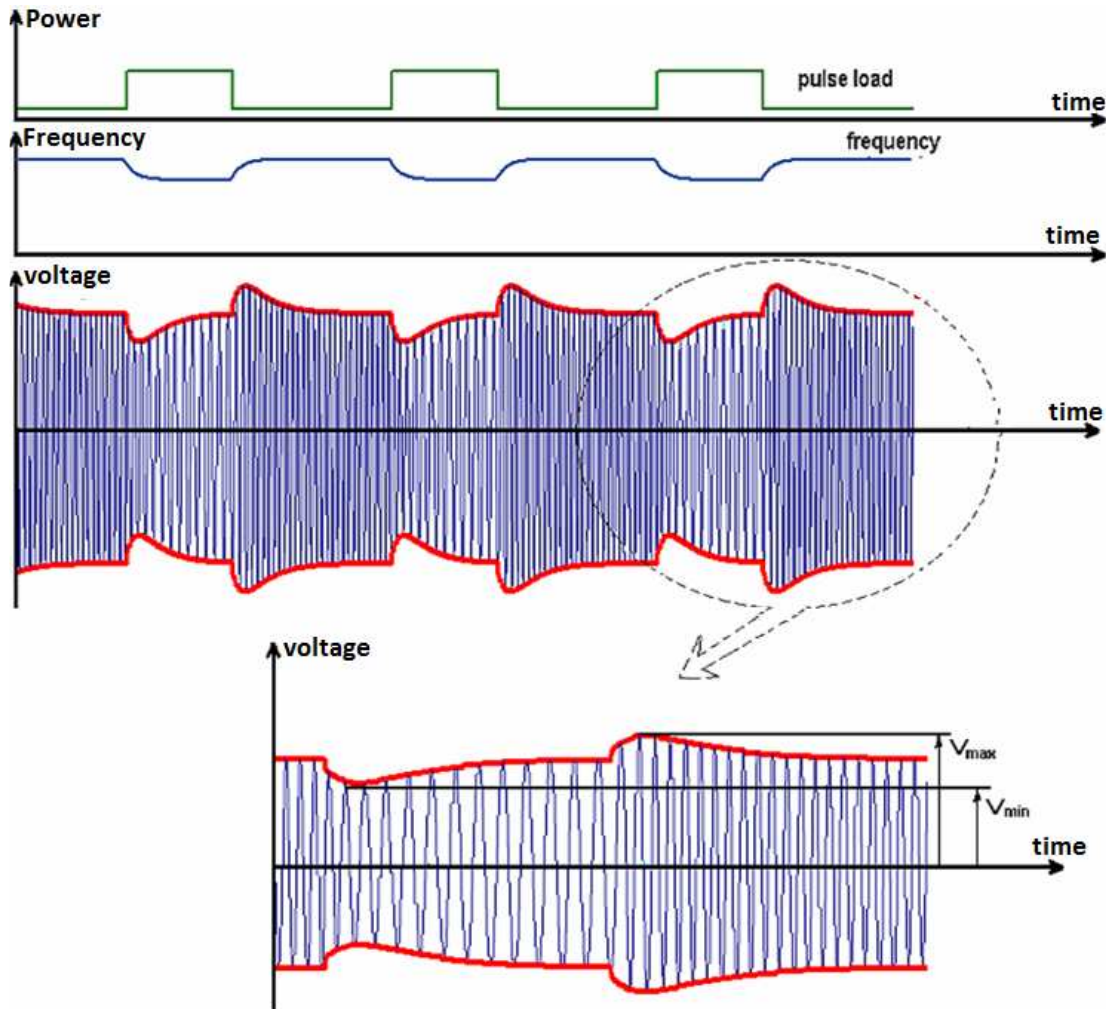

FIGURE 1. Frequency and voltage modulation provoked by a rectangular pulsed load.

Specifically, STANAG 1008 [8: Annex B § 9.d], design constraints are derived presuming that voltage/frequency modulation do not to exceed the above-mentioned limits if reactive and active power of the pulsed load satisfy the following inequalities:

$$\text{Voltage modulation: } \Delta Q < 0.065 \cdot S_S \qquad (3)$$

$$\text{Frequency modulation: } \Delta P < 0.25 \cdot S_S \qquad (4)$$

where *ΔP and ΔQ* are the active and the reactive power of the pulsed load respectively, S_S is the full rated apparent power of the supply at the occurrence of the pulsed load. Alternatively the inequalities (3) and (4) can be written as:

$$\text{Voltage modulation:} \quad \cos\phi > \sqrt{1 - \left(a \cdot \frac{1}{\Delta S}\right)^2} \; : \quad a = 0.065 \tag{5}$$

$$\text{Frequency modulation:} \quad \Delta S \cdot \cos\phi < \beta \; : \quad \beta = 0.25 \tag{6}$$

where ΔS is the apparent power of the pulsed load referred to the full rated apparent power of the supply at the occurrence of the pulsed load, thereinafter called *pulsed load relative apparent power*, $\cos\phi$ is the power factor of the pulsed load, *α* and *β* are the two parameters affecting the dimension of acceptable and unacceptable areas of operation; for STANAG they are fixed at 0.25 and 0.065, respectively.

In Fig. 2 the graphical representation of inequalities is shown, where the acceptable and unacceptable range of pulsed load installed capacity is highlighted.
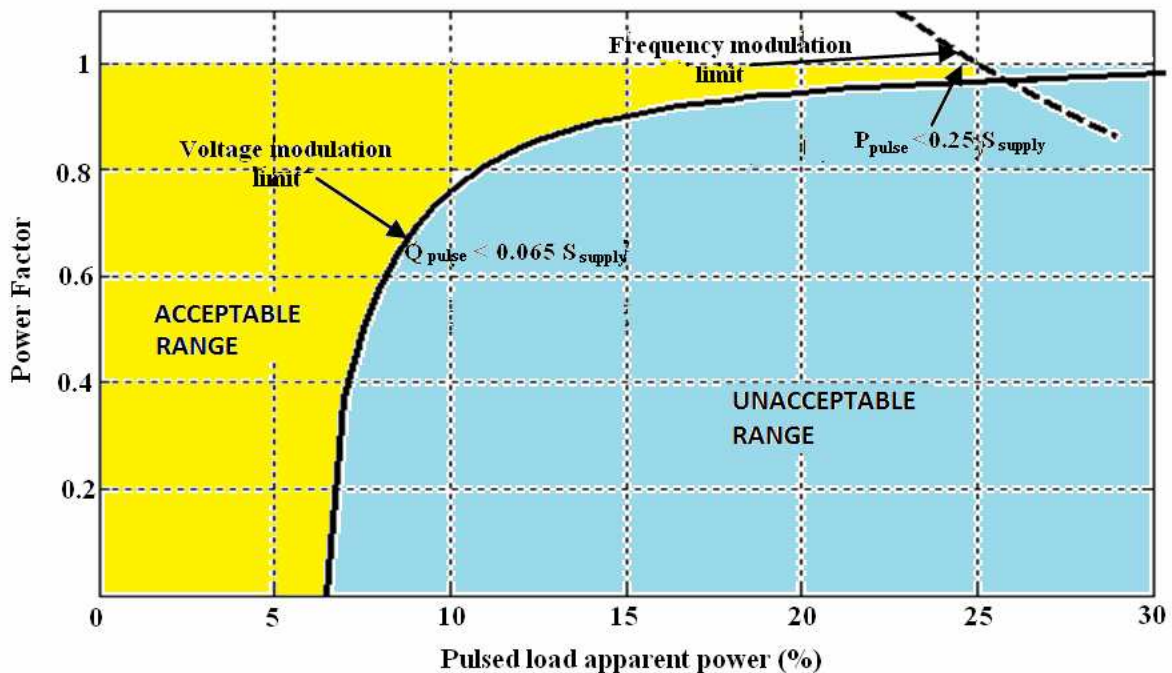

FIGURE 2. Limit curves for pulsed load operation according inequalities (5) and (6).

In a former work of the authors [10], a conventional ship electric system, comprising only low voltage electric power generation without electric propulsion, it was shown that STANAG 1008 guideline seems to be a method leading to a rather rough estimation of pulsed loads limits, as it considers only the pulsed load relative apparent power ΔS and the power factor of the pulsed load $\cos\phi$, but it does not take into account certain additional parameters affecting the entire phenomenon such as [2]:

- periodicity of modulation (pulse repetition frequency),
- duration of the pulsed load (duty cycle),
- profile of the pulsed load,
- point of connection of the pulsed load onto the electric grid,
- system impedance (such as cables equivalent impedance, generators sub-transient impedance etc.),

4

- operational characteristics of the generators and their associated frequency and voltage controllers,
- loading of the generator at the time of pulsed load occurrence.

In this paper, an effort is made to examine and validate the aforementioned STANAG 1008 design constraints in the frame of the All Ellectric Ship (AES) concept, where the AES includes high voltage (HV) electric power generation, low voltage (LV) ship service power supply system, HV electric propulsion, HV or LV pulsed loads. The voltage and frequency modulation in the LV sub-networks of an AES is studied via simulations in Matlab / Simulink [12], taking into account various parameters affecting the entire phenomenon such as: the periodicity, the duty cycle, the time-profile and the point of the connection of the pulsed load, the technical characteristics of the generators (like sub-transient reactance, intertia) and their associated frequency and voltage controllers (like governor and automatic voltage regulator (AVR) gains etc), the loading factor of the generator at the time of the pulsed load occurrence, the equivalent length of the cable between the pulsed load and the generator etc.

Thus, a simplified parametrical model of the electrical power system of a naval warship, comprising a pulsed load of rectangular profile (which is directly connected to the electric network), is developed, in order to study the phenomenon. Concerning the topology of the ship electric network, three different cases of power systems are considered:

- conventional, where the LV generator set supplies only a conventional service load and a pulsed load,
- AES with pulsed load in low voltage system, where the HV generator set supplies a HV propulsion load and a LV conventional service load along with a pulsed load,
- AES with pulsed load in high voltage system, where the HV generator set supplies a LV conventional service load and a HV propulsion load along with a pulsed load.

In all cases the pulsed load is directly connected to the electric network. Different simulations are run by varying several of the aforementioned parameters. The respective results are presented and the effects of the respective parameters on the pulsed load limit curve of STANAG 1008 are commented comparing the three different types of power systems examined.

Finally, general conclusions are derived for the effect of the aforementioned parameters on voltage/frequency modulation and on maximum acceptable pulsed load installed power. Moreover, suggestions are made for the improvement of the respective section of this standard.

TOPOLOGY OF THE SHIP ELECTRIC NETWORK

Next, the electric power systems of a conventional ship and an All Electric Ship are simplified as shown in Fig. 3, 4 and 5, without affecting the accuracy of the obtained results. In case of All Electric Ship pulse load is considered to be connected in low or high voltage systems as shown in Figs 4 and 5, respectively. The abbreviation "MP" represents the measurements points where voltage modulation is estimated.

The equivalent model of the conventional ship consists of:

- A generating set, which is aggregated in a 2 MVA, 440 V (low voltage) synchronous generator driven by diesel engine (equivalent to typical generating sets). The generator's parameters are summarized in Table 1.
- A low voltage network, which is aggregated in two three-phase sub-networks operating at 440 V and 115 V (the last one includes a 800 kVA, 440/115 V transformer of delta-star connection for its supply, where the transformer equivalent impedance is 0.008+j·0.04 p.u.). The equivalent impedance of the cable of the first sub-network is equal to

0.03+j·0.07 Ohm/km, while the respective one of the second sub-network is equal to 0.05 +j·0.175 Ohm/km referred to 440 V system. The respective lengths are L_{440} and L_{115}, and they are considered as variables.

- A service load, which is divided into two parts: 440 V service load and 115 V service load using the factor n_{LV440}, which is the fraction between the apparent power of 440 V service load and the respective one of the total service load. The power factor equals to 0.80 for the base scenario.
- A pulsed load of rectangular profile, as it is shown in Fig. 6, which is connected to the 440 V network.
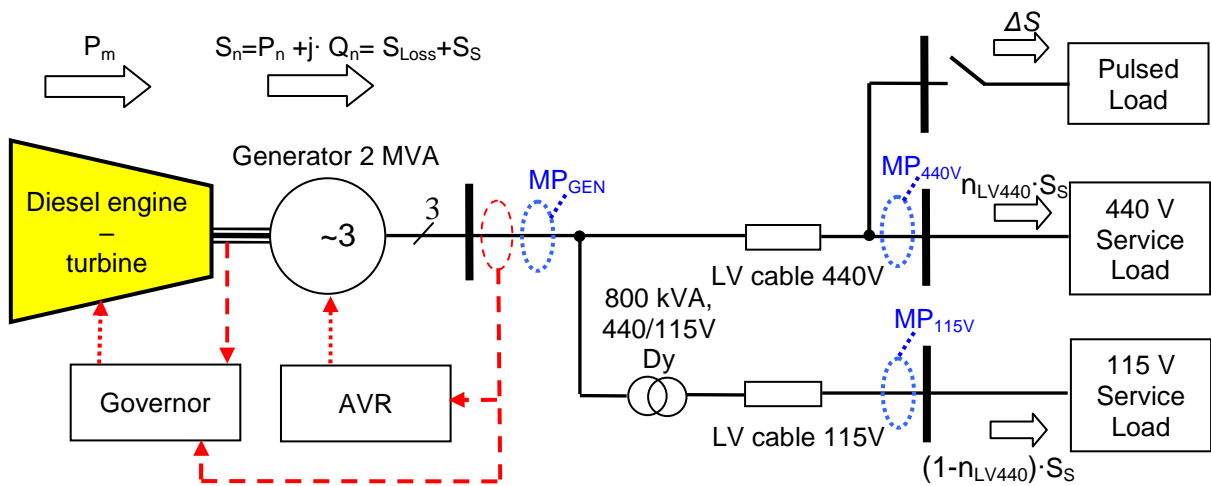
FIGURE 3. Equivalent topology of a conventional ship electric power system.
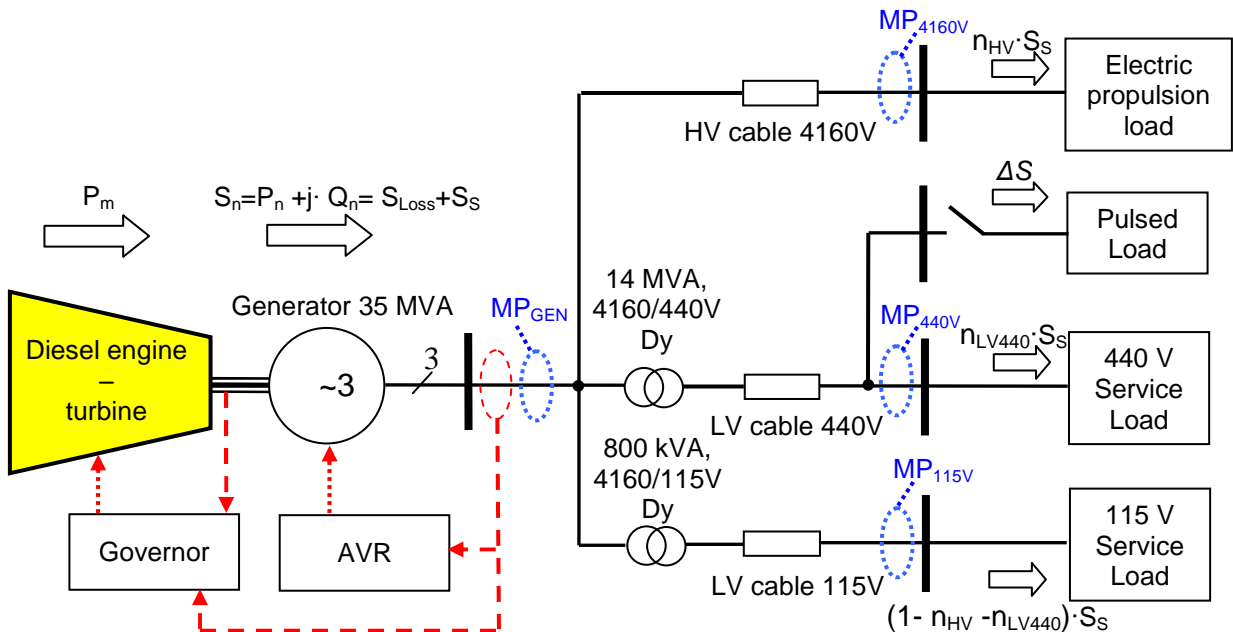
FIGURE 4. Equivalent topology of an AES electric power system with pulsed load in LV 440 V network.

6
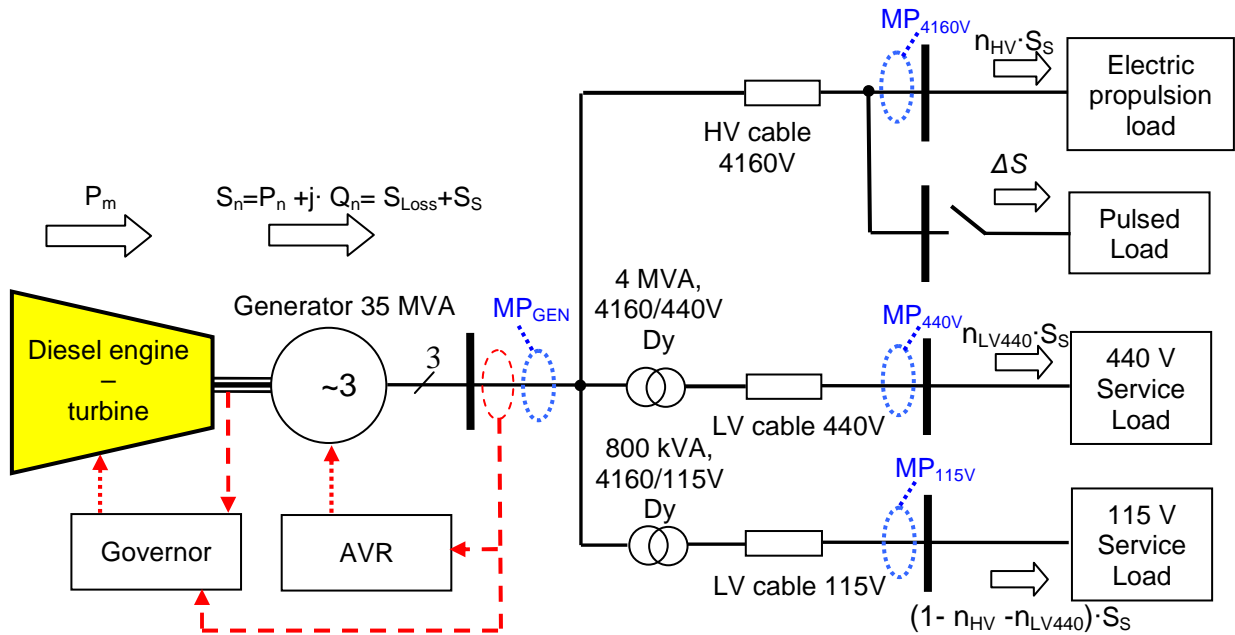
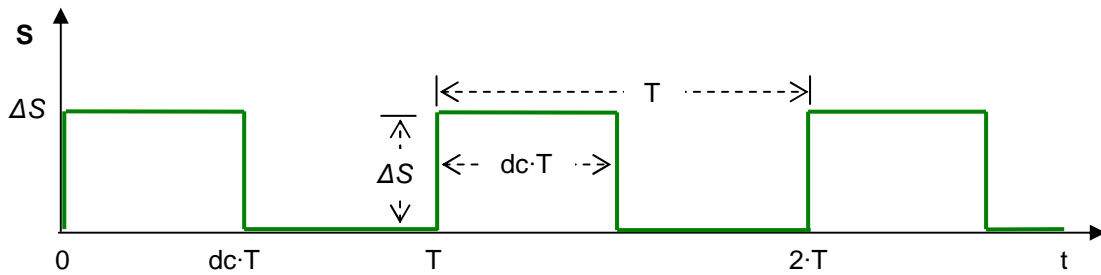**FIGURE 5.** Equivalent topology of an AES electric power system with pulsed load in HV 4160 V network.

FIGURE 6. Pulsed load typical profile.

TABLE (1). Generator's typical technical data for different topologies.

Ship power system Parameter	Conventional	AES with pulsed load in LV network	AES with pulsed load in HV network
		Values	
S_n (MVA)	2	35	35
V_n (V)	440	4160	4160
r_a (p.u.)	0.0036	0.00285	0.00285
X_d (p.u.)	1.56	1.305	1.305
X'_d (p.u.)	0.296	0.296	0.296
X''_d (p.u.)	0.177	0.150	0.150
X_q (p.u.)	1.06	0.475	0.475
X''_q (p.u.)	0.177	0.150	0.150
X_l (p.u.)	0.052	0.180	0.180
T'_{do} (sec)	3.7	1.7	1.7
T''_{do} (sec)	0.05	0.05	0.05
T''_{qo} (sec)	0.05	0.1	0.1
H (sec)	1.07	1.5	1.5
F (p.u.)	0.1	0.1	0.1
Pole pairs (-)	4	4	4

The equivalent model of the AES with pulse load in low voltage system consists of:

- A generating set, which is aggregated in a 35 MVA, 4160 V (high voltage) synchronous generator driven by diesel engine (equivalent to typical generating sets). The generator's parameters are summarized in Table 1.
- A high voltage network of 4160 V, which supplies the electric propulsion. Cable impedance is equal to 0.0375+j·0.0875 Ohm/km. The respective length is L_{HV}.
- A low voltage network, which is aggregated in two three-phase sub-networks of 440 V and 115 V. Each one uses a transformer of delta-star connection for its supply (14 MVA, 4160/440 V for the first one and 800 kVA, 4160/115 V for the second one, while the equivalent impedance for all cases is 0.01+j·0.05 p.u. of each transformer). Cable impedance of the first sub-network is equal to 0.075+j·0.175 Ohm/km, while the respective one of the second sub-network is equal to 0.15 +j·0.35 Ohm/km, all referred to 4160 V system. The respective lengths are L_{LV440} and L_{LV115}, which are considered as variables.
- A service load, which is divided into three parts: 4160 V electric propulsion load, 440 V conventional service load and 115 V conventional service load. They are defined by the factors n_{HV} and n_{LV440}, which are the fractions between the apparent power of the propulsion load and the respective one of the total service load, and between the apparent power of 440 V service load and the respective one of the total service load. The power factor is constant and equal to 0.75.
- A pulsed load of rectangular profile, as it is shown in Fig. 6, which is connected to the 440 V network.

The equivalent model of the AES with pulse load in high voltage system consists of:

- A generating set, which is aggregated in a 35 MVA, 4160 V (high voltage) synchronous generator driven by diesel engine, similar to the respective one of AES with pulse load in low voltage system.
- A high voltage network of 4160 V, which supplies the electric propulsion. Cable impedance is equal to 0.0375+j·0.0875 Ohm/km. The respective length is L_{HV}.
- A low voltage network, which is aggregated in two three-phase sub-networks of 440 V and 115 V, similar to the respective one in case of AES with pulse load in low voltage system, except the 4160/440 V transformer, with 4 MVA nominal apparent power instead of 14 MVA.
- A service load, which is similar to the respective one of AES with pulse load in low voltage system.
- A pulsed load of rectangular profile, as it is shown in Fig. 6, which is connected to the 4160 V network.

The generator control system consists of the governor system and the automatic voltage regulator (AVR) and is similar in the three electrical systems. The respective block diagrams are shown in Fig. 7 and 8, while the respective parameters are summarized in Table 2.
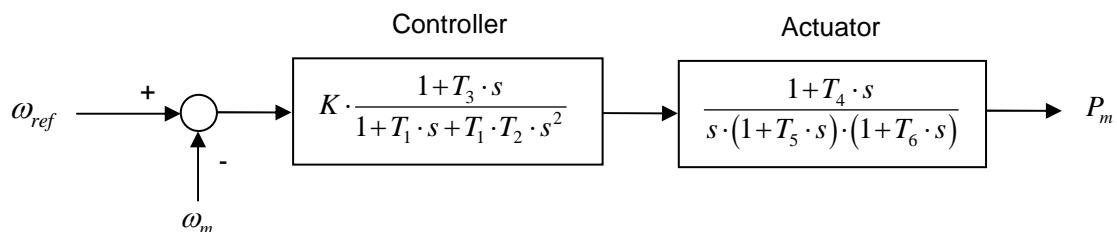

FIGURE 7. Governor block diagram, where ω_{ref} is the reference rotating speed, ω_m the measured rotating speed, P_m the mechanical power.
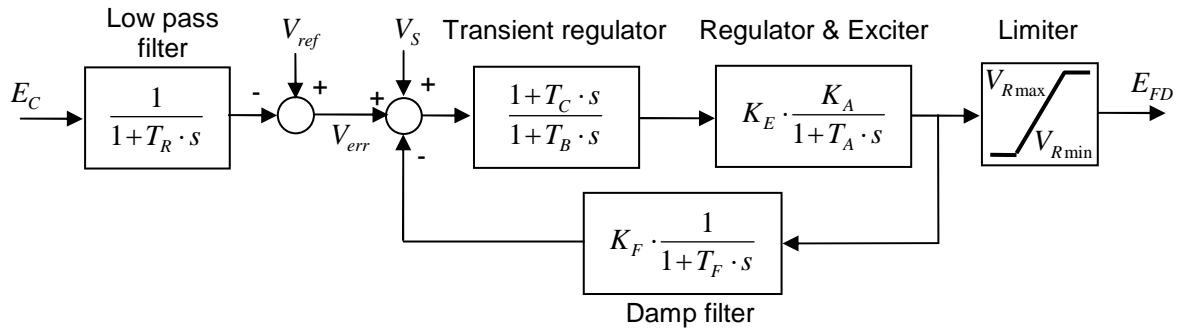
FIGURE 8. Automatic Voltage Regulator block diagram, where E_{FD} is the field voltage reference, V_{ref} the voltage reference, V_S the stabilization voltage signal, V_{err} the error voltage, E_C the measured voltage.

TABLE (2). Parameters of the governor and AVR according to the block diagrams of Fig. 7, 8.

Governor		AVR	
Parameter	**Value**	**Parameter**	**Value**
K	40	**K_A**	200
T_1 (sec)	0.01	**K_E**	1
T_2 (sec)	0.02	**K_F**	0.001
T_3 (sec)	0.2	**T_A (sec)**	0.001
T_4 (sec)	0.25	**T_B (sec)**	0
T_5 (sec)	0.009	**T_C (sec)**	0
T_6 (sec)	0.0384	**T_F (sec)**	0.1
		T_R (sec)	0.020
		V_{Rmax} (p.u.)	6.0
		V_{Rmin} (p.u.)	-6.0

Indicative results concerning repetitive pulsed load application are shown in Fig. 9 for the basic operation scenario of AES with the pulsed load installed at the high voltage system. The generator active power, the system frequency, the root mean square (RMS) voltages at the generator bus, the high voltage bus, the 440V service load bus and the 115V service load bus are presented.

Basic scenario includes the following assumptions: initial service base load is 0.40 p.u. (divided in 85% in high voltage-propulsion service load, 10% in 440 V service load and 5% in 115V service load), the system frequency is 60 Hz, the equivalent length is 100 m for each network cables, while the pulsed load apparent load equals 0.10 p.u., the respective duty cycle 50% and the respective period 0.3 sec. It is noted that the pulsed load is activated at 0.5 sec for first time.

It is obvious from Fig. 9 (a) to 9 (c) that immediately after pulsed load application a sub-transient phenomenon occurs which should be included in voltage/frequency modulation estimation. The governor and the automatic voltage regulator are trying to stabilize the frequency and the voltage close to their nominal values, but the pulsed load causes significant deviations. The patterns of the voltage at the load buses follow the respective one of the generator bus voltage but with smaller mean values.
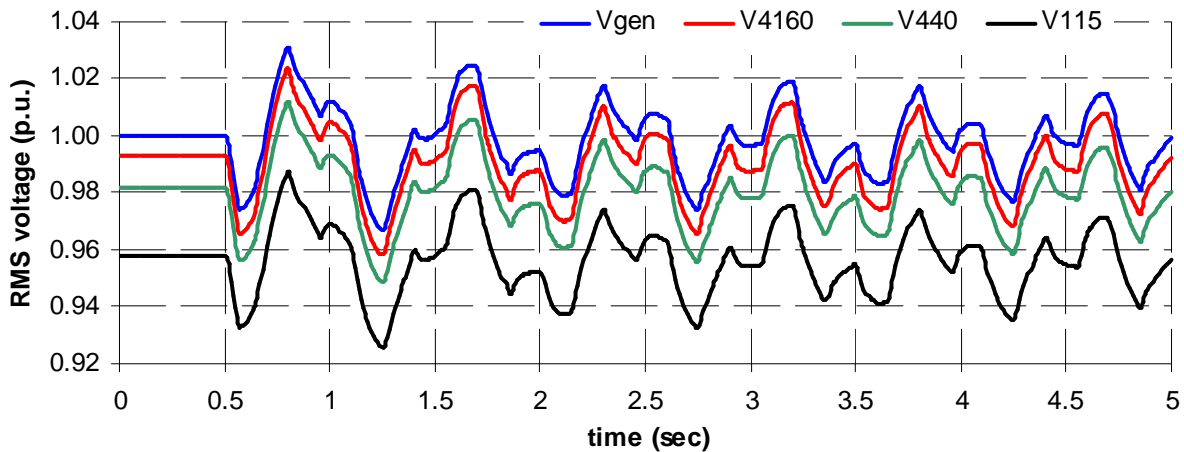
Similar results can be obtained from the other two topologies.

9
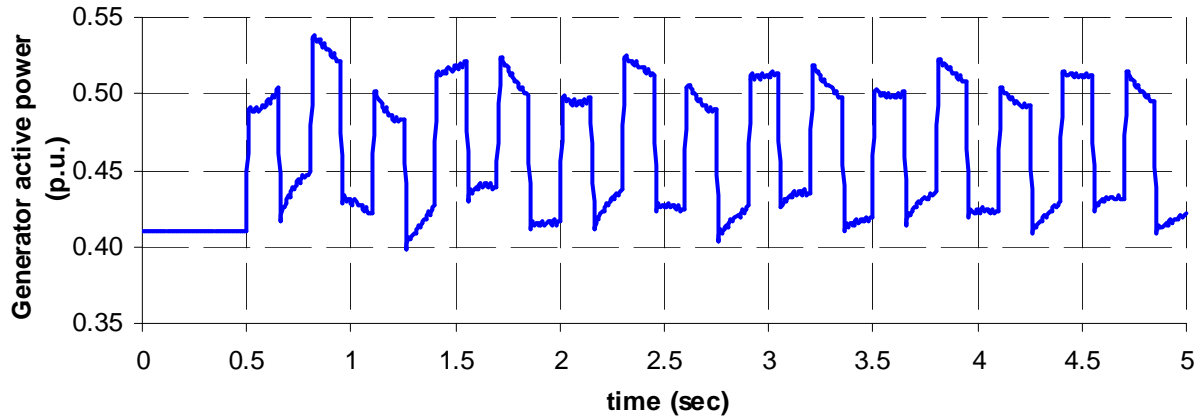
(a)
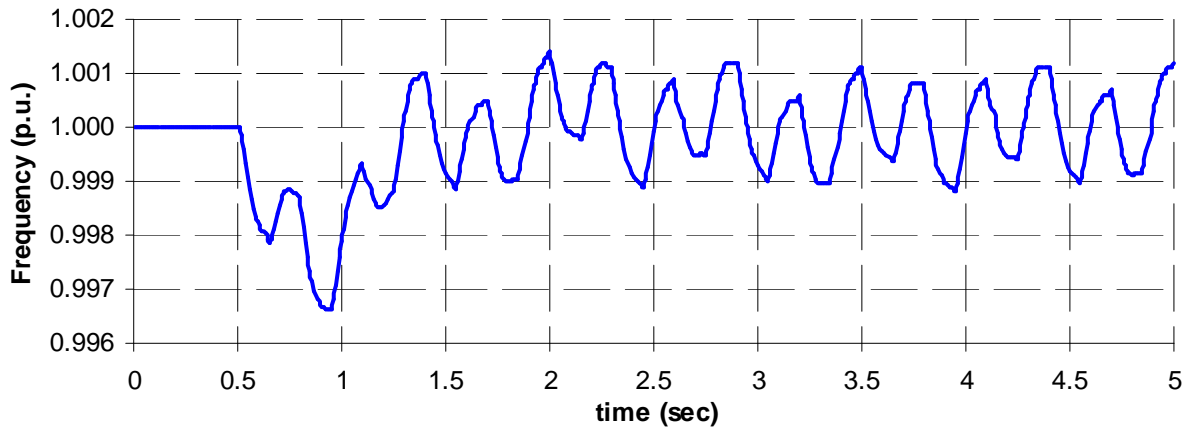
(b)

(c)

FIGURE 9. (a) Generator active power, (b) frequency, (c) root mean square (RMS) voltages at the generator bus (Vgen), the high voltage bus (V4160), the 440V low voltage bus (V440) and the 115V low voltage bus (V115) vs time for the basic operation scenario of AES with pulsed load in HV network (Service base load = 0.40 p.u., system frequency = 60 Hz, Pulsed load apparent load = 0.10 p.u., duty cycle = 50%, pulsed load period = 0.3 sec, L_{HV}= L_{LV440} =L_{LV115}=100 m, n_{HV} =0.85 and n_{LV440}=0.10).

SIMULATION RESULTS FOR THE THREE DIFFERENT TOPOLOGIES OF THE SHIP ELECTRIC NETWORK

The electrical networks shown in Fig. 3, 4, 5 are simulated for different operating scenarios with a rectangular pulsed load. The obtained results concerning pulsed load limits are compared with the power factor – pulsed load apparent power limit curve proposed by STANAG 1008 (inequalities (5), (6) and Fig. 2). The standard voltage / frequency modulation limits, 2%, 0.5% are considered for all examined operating scenarios and network topologies measured and are measured at 440 V low voltage service load bus. Typical operation parameters of the basic scenario for each ship topology are presented in Table 3.

TABLE (3). Typical values of operation parameters of the basic scenario for each ship topology.

Ship power system Parameter	Conventional [2]	AES with pulsed load in LV network Values	AES with pulsed load in HV network
Service load factor of the generator (without losses) at the time of the pulsed load occurrence n_{serv} (-)	0.50	0.40	0.40
Ratio of HV service load apparent power to the total one n_{HV}	- (no existence)	0.85	0.85
Ratio of 440V service load apparent power to the total one n_{LV440}	0.75	0.10	0.10
Ratio of 115V service load apparent power to the total one n_{LV115}	0.25	0.05	0.05
Service load power factor (-)	0.80	0.80	0.80
HV cable equivalent length L_{HV} (m)	- (no existence)	100	100
440V cable equivalent length L_{440}(m)	100	100	100
115V cable equivalent length L_{115}(m)	50	100	100
Pulsed load period (sec)	0.3	0.3	0.3
Pulsed load duty cycle (%)	50	50	50
Generator's sub-transient reactance $X_d{}^/=X_q{}^/$ (p.u.)	0.177	0.150	0.150
Generator's inertia H (sec)	1.07	1.50	1.50
Governor's gain K (-)	40	40	40
AVR gain K_A (-)	200	100	200
Generator's field voltage upper bound V_{Rmax} =- V_{Rmin} (p.u.)	5.0	6.0	6.0

The time-profile of the pulsed load is rectangular, because other shapes such as triangular etc, lead on milder transient phenomena and smaller modulation effects for the same peak apparent power, duty cycle and period. Pulsed load can be connected either to the high voltage network or to the 440 V low voltage network. The 115V low voltage has already been excluded for all examined topologies, because the pulsed load strains the respective equipment hard. Generally, only one basic parameter is changed and the rest are maintained constant, examining in this way the extent that the specified parameter affects the results. Before any of the following simulations the system is initialized properly and then it is simulated for a time interval of 2.5 sec (except for cases that pulsed load period greater than 0.6sec is examined) iteratively for different pairs of values of apparent power and power factor of the pulsed load, until STANAG 1008 modulation limits are reached. In this way the actual corresponding power factor – pulsed load apparent power curve point is determined. It is noted that the usual values of the parameters almost always activate the voltage modulation inequality.

Following, a sensitivity analysis of each parameter is provided separately.

Service Load Factor of the Generator
at the Time of the Pulsed Load Occurrence

The service load factor of the generator before the application of the pulsed load is considered as a parameter. Specifically, this parameter takes into account only the service load in any network, without the losses of the cables and of the windings of the generator and the transformers. Because of the losses of the system the mechanical input power of the diesel engine will be slightly bigger than the power of the service load.

For the case of the AES with the pulsed load in HV network, service loads of 5%, 10%, 20%, 30%, 40% (basic scenario), 50%, 60%, 70%, 80% are considered and the system is simulated repeatedly, so that the respective power factor – pulsed load apparent power curves are extracted, as shown in Fig. 10. It is obvious that the increase of the base load tends to decrease the unacceptable operation area for small values of service load (between 10% and 30%). For very small values (as 5%) or big values (above 40%) the unacceptable operating area increases making the respective curve of STANAG 1008 quite insufficient. This does not happen for all respective values, i.e. 60%, due to the non-linear behavior of voltage / frequency modulation with the service load factor.
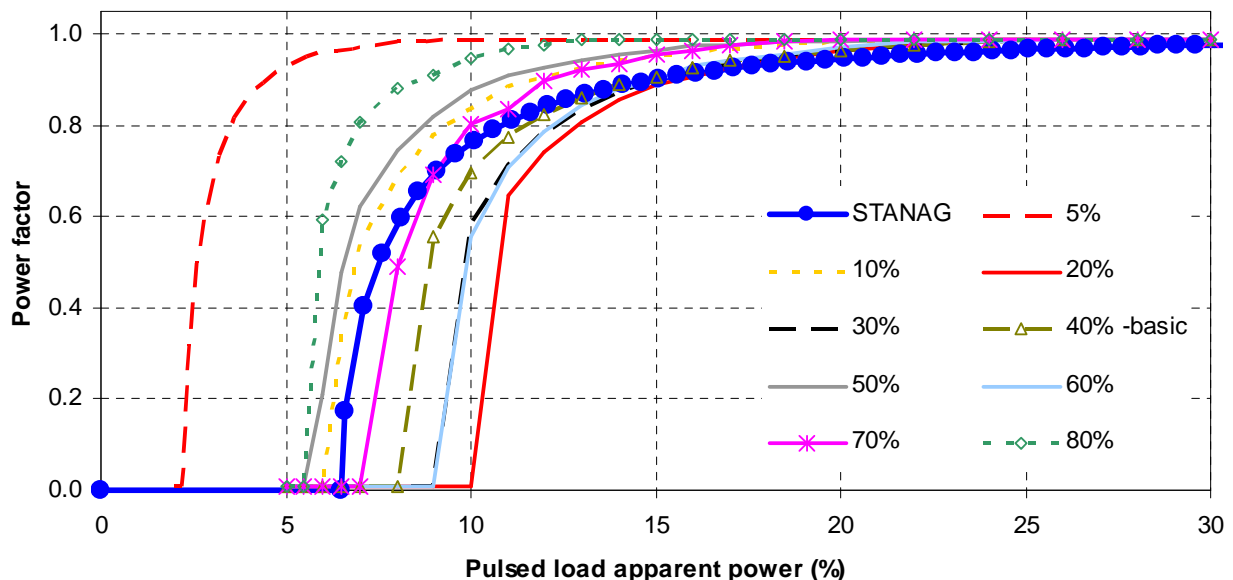
FIGURE 10. Power factor vs pulse load apparent power for different values of the service load factor of the generator in the case of the AES with pulsed load in HV network.

In case of the AES with the pulsed load installed at LV network, the system is simulated repeatedly for 5%, 10%, 20%, 30%, 40%, 50%, 60%, 70%, 80% service base loads and the respective curves are extracted, as it is shown in Fig. 11. It is obvious that the respective curve and the unacceptable operating area are underestimated in STANAG 1008. However, the respective curves are located in a narrower area than the previous ones of Fig. 10.

For the case of the conventional ship, as the authors have already mentioned in [2] and as it is shown in Fig. 12, the increase of the base load tends to decrease the unacceptable operating area. In this case the unacceptable operating area of the respective STANAG 1008 curve is quite sufficient.
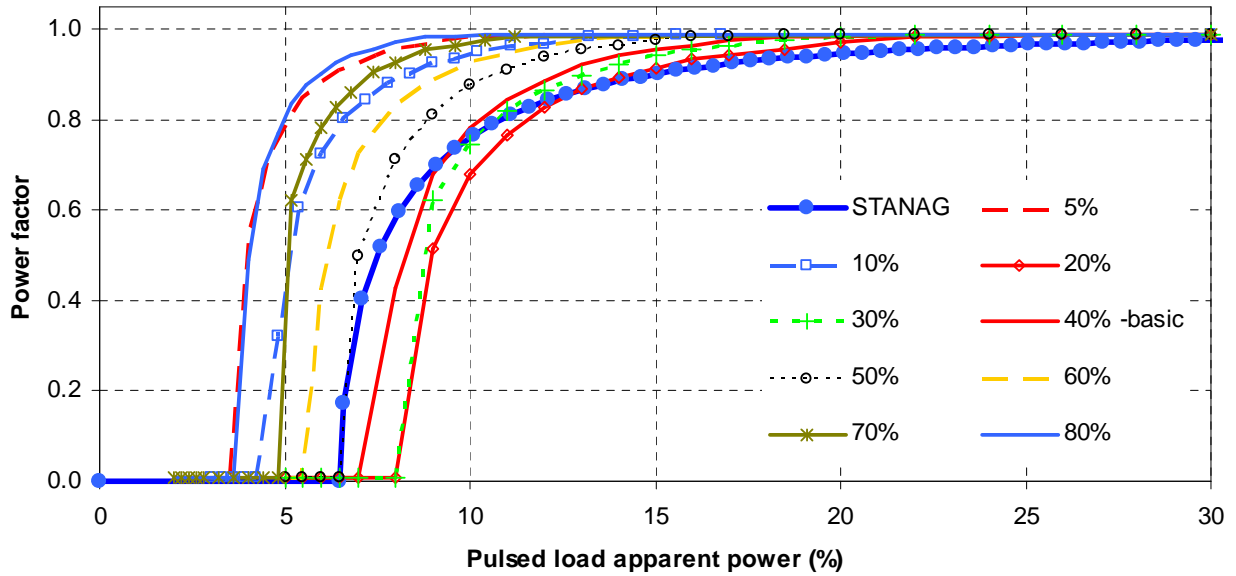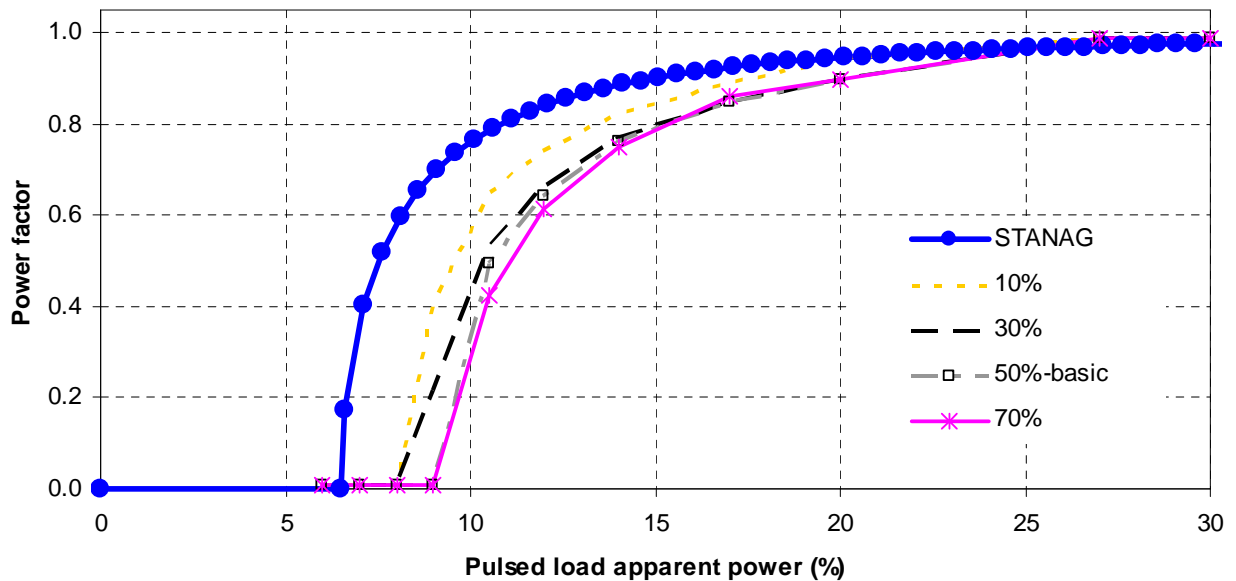
FIGURE 11. Power factor vs pulse load apparent power for different values of the service load factor of the generator in the case of the AES with pulsed load in LV network.

FIGURE 12. Power factor vs pulse load apparent power for different values of the service load factor of the generator in the case of the conventional ship [2, Fig.7].

Service Load Distribution to Different Voltage Networks

For the two topologies of the AES the electric service load is distributed into three different voltage networks according to the following ratios:

- the ratio n_{HV} of the HV service load apparent power to the total service load apparent power,

13

- the ratio n_{LV440} of the 440V low voltage service load apparent power to the total service load apparent power,
- the ratio n_{LV115} of the 115V low voltage service load apparent power to the total service load apparent power.

It is noted that the total apparent power of the service load does not take into account the losses of the cables and of the windings of the generator and the transformers. So the three ratios are connected by the following equation:

$$n_{HV} + n_{LV440} + n_{LV115} = 1 \qquad (7)$$

It is obvious that two ratios of the three ones can be independent parameters. The third ratio is calculated by eq. (7).

Similarly, in the case of the conventional ship only the ratios n_{LV440} and n_{LV115} are defined, while the respective equation is:

$$n_{LV440} + n_{LV115} = 1 \qquad (8)$$

In eq. (8) only one ratio is the free parameter.

For the case of the AES with the pulsed load installed at HV network, first it is assumed that the ratio n_{LV115} is constant and equal to 5%, while the ratio n_{HV} of the service load in the HV network takes the values 60%, 65%, 70%, 75%, 80%, 85% (basic scenario) and 90%. Respectively the ratio n_{LV440} of the service load in the 440V LV network is calculated by eq. (7). For the above values of the ratio n_{HV} the equivalent model is simulated repeatedly and the respective power factor – pulsed load apparent power curves are obtained, as it is shown in Fig. 13. It is obvious that the increase of the ratio n_{HV} of the HV service load, with the respective ratio n_{LV115} of the 115V LV service load to be constant, tends to increase the unacceptable operating area slightly.
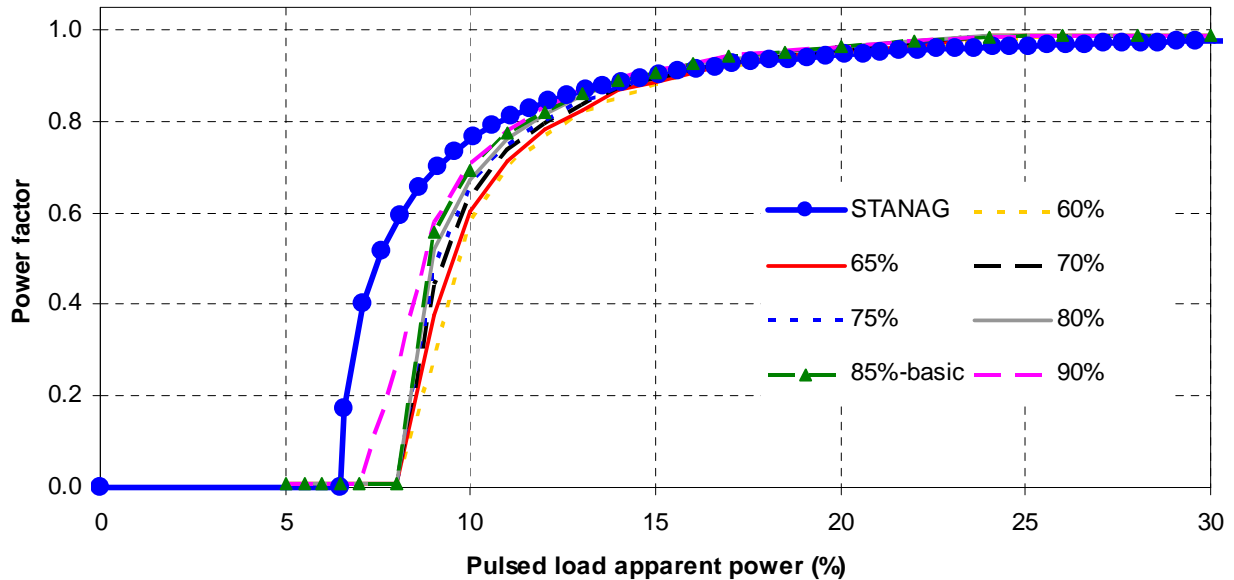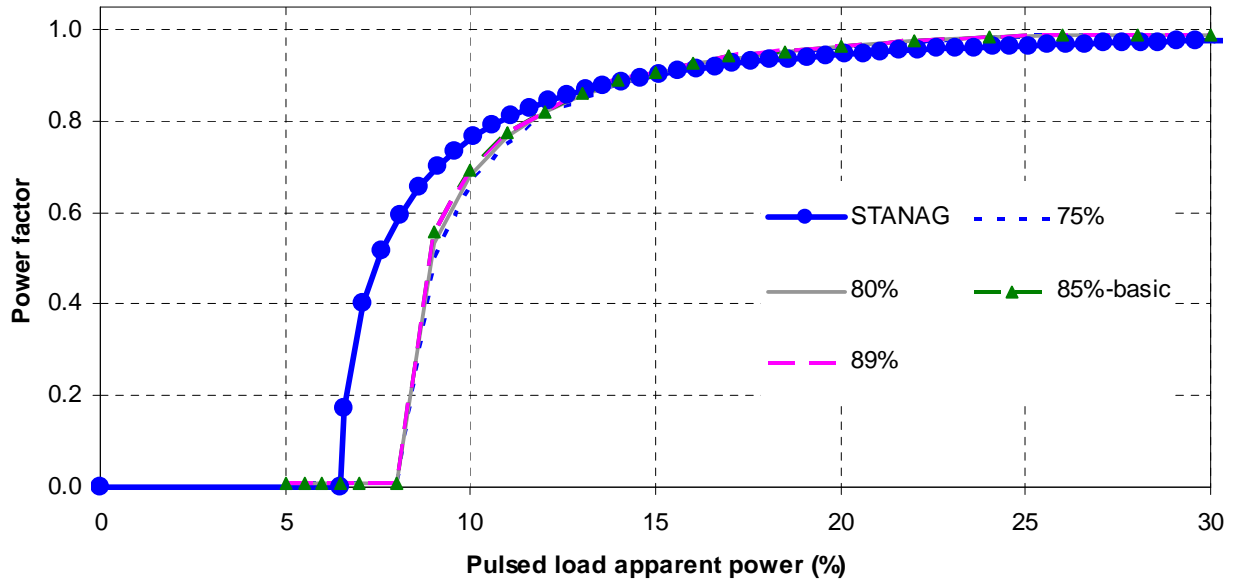

FIGURE 13. Power factor vs pulse load apparent power for different values of the ratio n_{HV} of the HV service load apparent power to the service load apparent power with constant the ratio n_{LV115} of the 115V LV service load apparent power to the service load apparent power and equal to 5% in the case of the AES with pulsed load in HV network.

14

In the second step it is assumed that the ratio n_{LV440} is constant and equal to 10%, while the ratio n_{HV} of the service load in the HV network is equal to 75%, 80%, 85% (basic scenario), 89%. Respectively the ratio n_{LV115} of the service load in the 115V LV network is calculated by eq. (7) to be equal to 15%, 10%, 5% (basic scenario), 1%. For the above values of the ratio n_{HV} the equivalent model is simulated repeatedly and the respective power factor – pulsed load apparent power curves are obtained, as it is shown in Fig. 14. It is obvious that the increase of the ratio n_{HV} of the HV service load, with the respective ratio n_{LV440} of the 440V LV service load to be constant, tends to increase the unacceptable operating area very slightly.

FIGURE 14. Power factor vs pulse load apparent power for different values of the ratio n_{HV} of the HV service load apparent power to the service load apparent power with constant the ratio n_{LV440} of the 440V LV service load apparent power to the service load apparent power and equal to 10% in the case of the AES with pulsed load in HV network.

For the case of the AES with the pulsed load installed at LV network in the first step it is assumed that the ratio n_{LV115} is constant and equal to 5%, while the ratio n_{HV} of the service load in the HV network is equal to 75%, 80%, 85% (basic scenario), 89%. The respective power factor – pulsed load apparent power curves are extracted, as it is shown in Fig. 15. The increase of the ratio n_{HV} of the HV service load, with the respective ratio n_{LV115} to be constant, tends to increase the unacceptable operating area slightly. Next, it is assumed that the ratio n_{LV440} is constant and equal to 10%, while the ratio n_{HV} varies between 75% and 89%. The respective curves are extracted and they are presented in Fig. 16. It is obvious that these curves are practically the same, which means that there is zero effect in the modulation phenomenon. Meanwhile there is a minor overlap of the unacceptable operating area determined by the STANAG 1008 curve.

For the case of the conventional ship, the examined values if the ratio n_{LV440} of the service load in the 440V LV network are 30%, 75% (basic scenario), 90%. Respectively the ratio n_{LV115} of the service load in the 115V LV network is calculated by eq. (8). The equivalent model is simulated repeatedly and the respective power factor – pulsed load apparent power curves are extracted, as it is shown in Fig. 17. It is obvious that the increase of the ratio n_{LV440} of the 440V LV service load tends to decrease the unacceptable operating area very slightly.
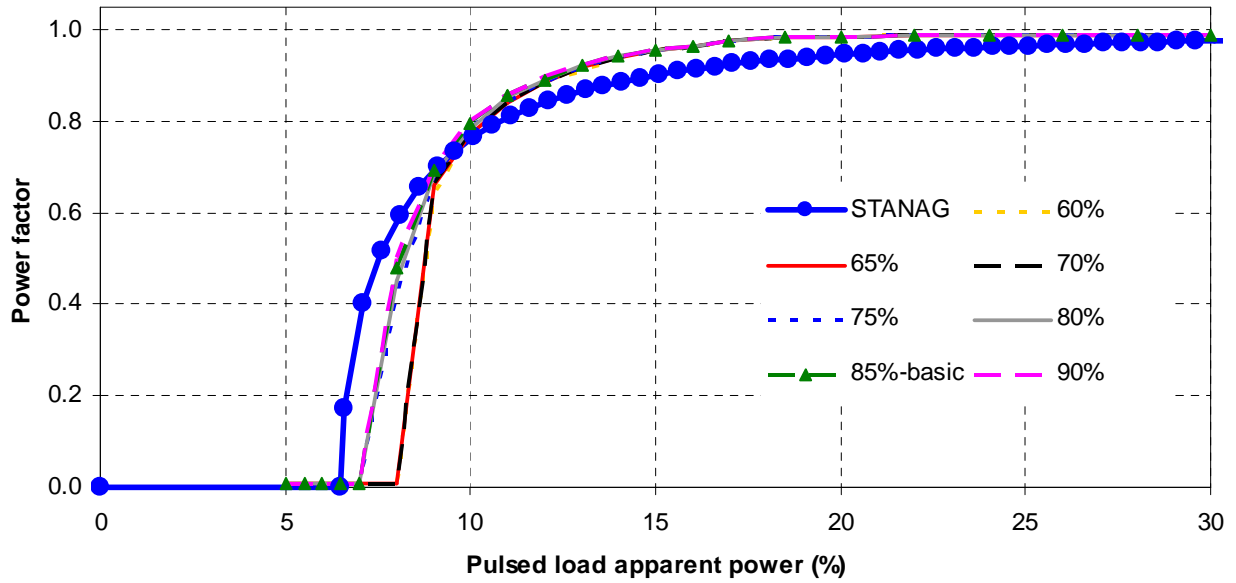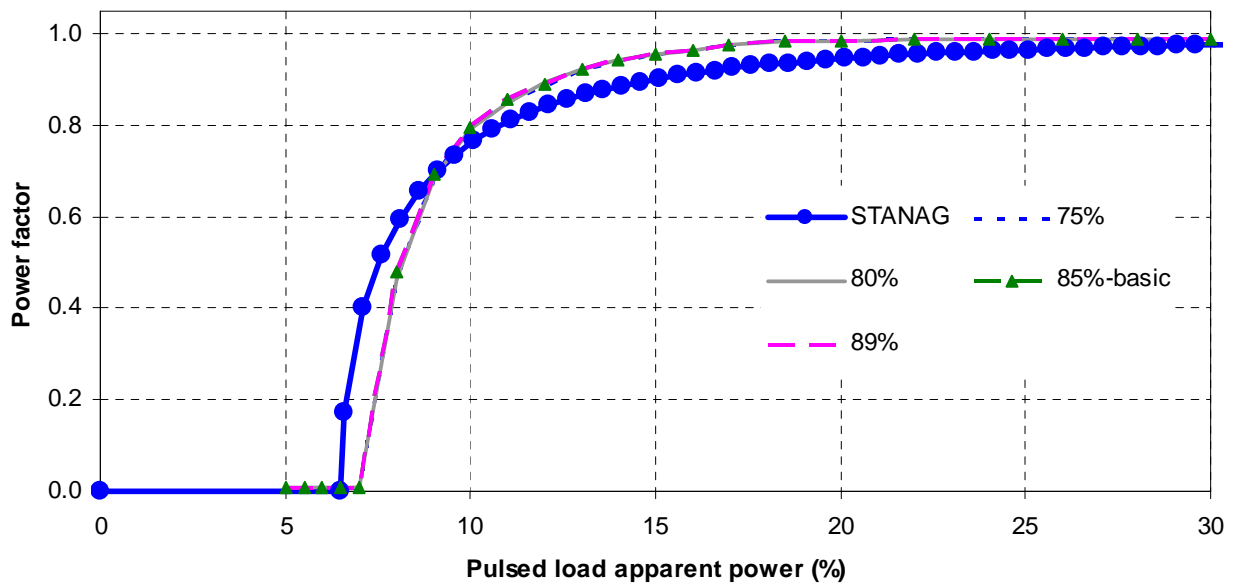
FIGURE 15. Power factor vs pulse load apparent power for different values of the ratio n_{HV} of the HV service load apparent power to the service load apparent power with constant the ratio n_{LV115} of the 115V LV service load apparent power to the service load apparent power and equal to 5% in the case of the AES with pulsed load in LV network.
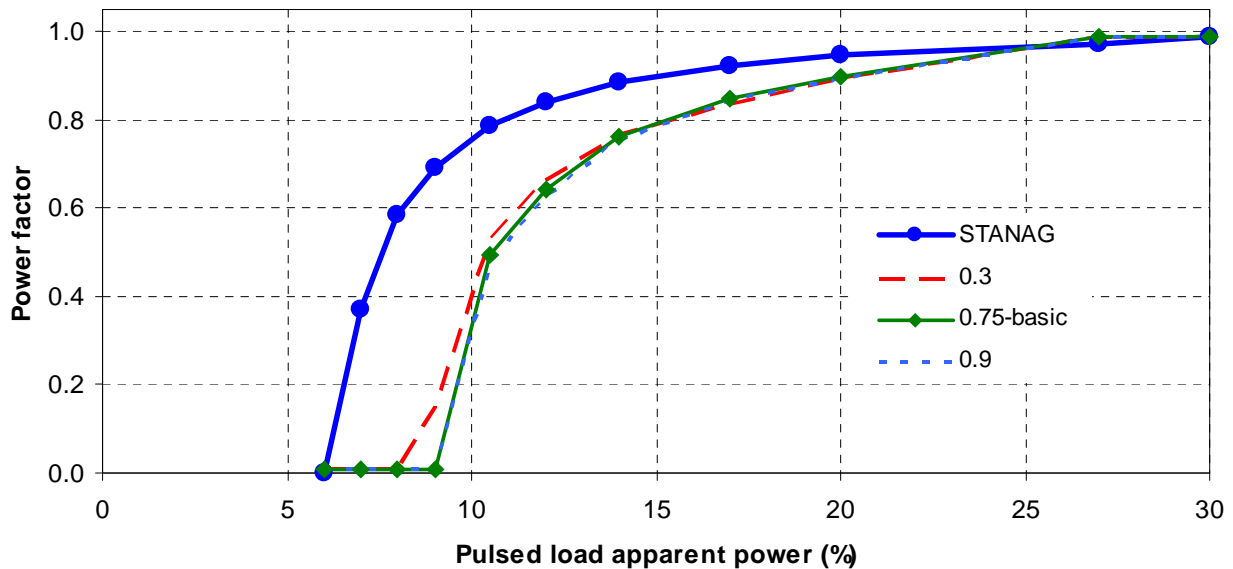

FIGURE 16. Power factor vs pulse load apparent power for different values of the ratio n_{HV} of the HV service load apparent power to the service load apparent power with constant the ratio n_{LV440} of the 440V LV service load apparent power to the service load apparent power and equal to 10% in the case of the AES with pulsed load in LV network.

16

FIGURE 17. Power factor vs pulse load apparent power for different values of the ratio n_{LV440} of the 440V LV service load apparent power to the service load apparent power in the case of the conventional ship.

Service Load Power Factor

In the previous cases the power factor of the service load in all sub-networks has been considered equal to 0.80 and inductive because of the inductive behavior of the motors and of the fluorescent lamps. Next different values of inductive power factor are examined.

For the case of the AES with the pulsed load installed at LV network, the respective power factor – pulsed load apparent power curves are extracted for different values of the inductive power factor (0.60, 0.707, 0.80 (basic scenario), 0.90 and 0.98) and they are presented in Fig. 18. It is obvious that the increase of the power factor of the service load tends to decrease the unacceptable operating area significantly, until the power factor reaches up to 0.90. Afterwards, the further increase of the power factor increases the respective area. In this case the respective curve of STANAG 1008 is quite insufficient for pulsed load power factor smaller than 0.80 and for service load power factor smaller than 0.80.

Similarly, for the case of the AES with the pulsed load installed at HV network, the respective curves are extracted for different values of the inductive power factor (between 0.70 and 0.90) and they are presented in Fig. 19. It is observed that the variation of the power factor of the service load above 0.80 tends to increase the unacceptable operating area significantly. The respective curves of the power factor are overlapped the curve of STANAG 1008.

For the case of the conventional ship the respective curves are extracted for different inductive power factors (between 0.70 and 1.00) and they are presented in Fig. 20. It is observed again that the increase of the power factor of the service load tends to increase the unacceptable operating area significantly. The respective curves of power factor are overlapped the curve of STANAG 1008 slightly for service load power factor 1.00 and pulsed load power factor bigger than 0.95.

For the aforementioned analysis it is clear that the power factor of the service load affects significantly the modulation.
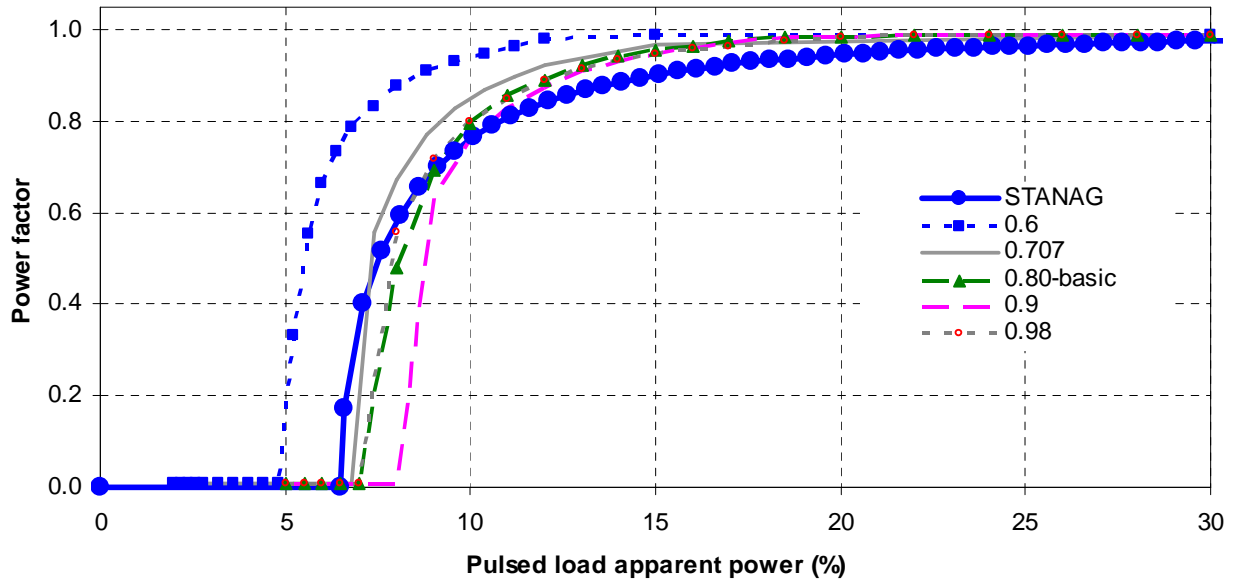
17

FIGURE 18. Power factor vs pulse load apparent power for different values of the service load power factor in the case of the AES with pulsed load in LV network.
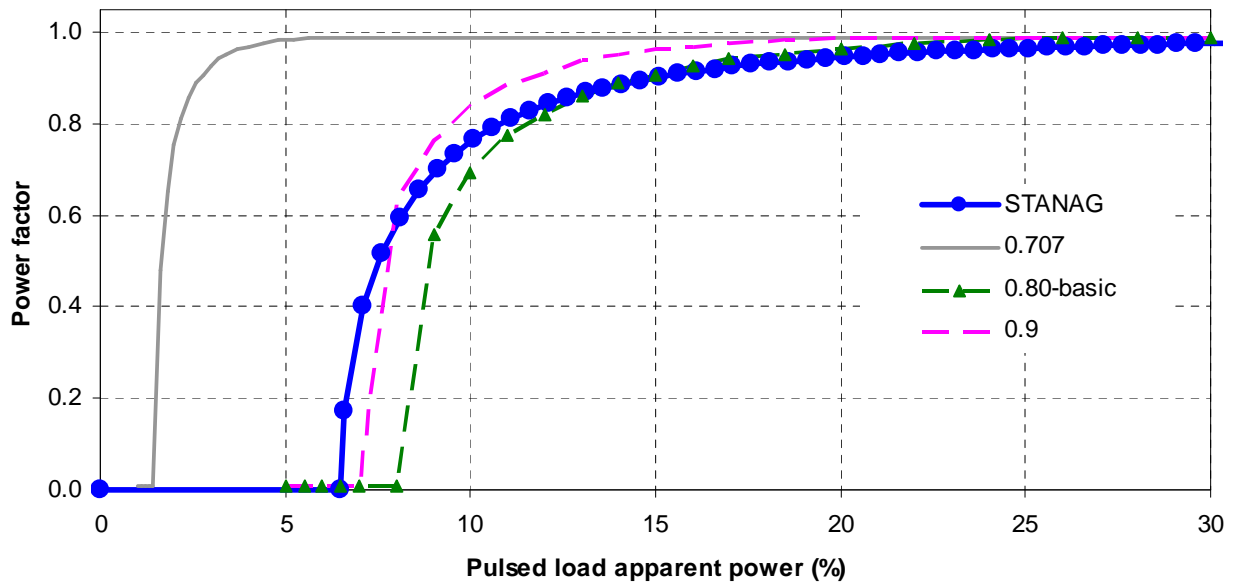

FIGURE 19. Power factor vs pulse load apparent power for different values of the service load power factor in the case of the AES with pulsed load in HV network.
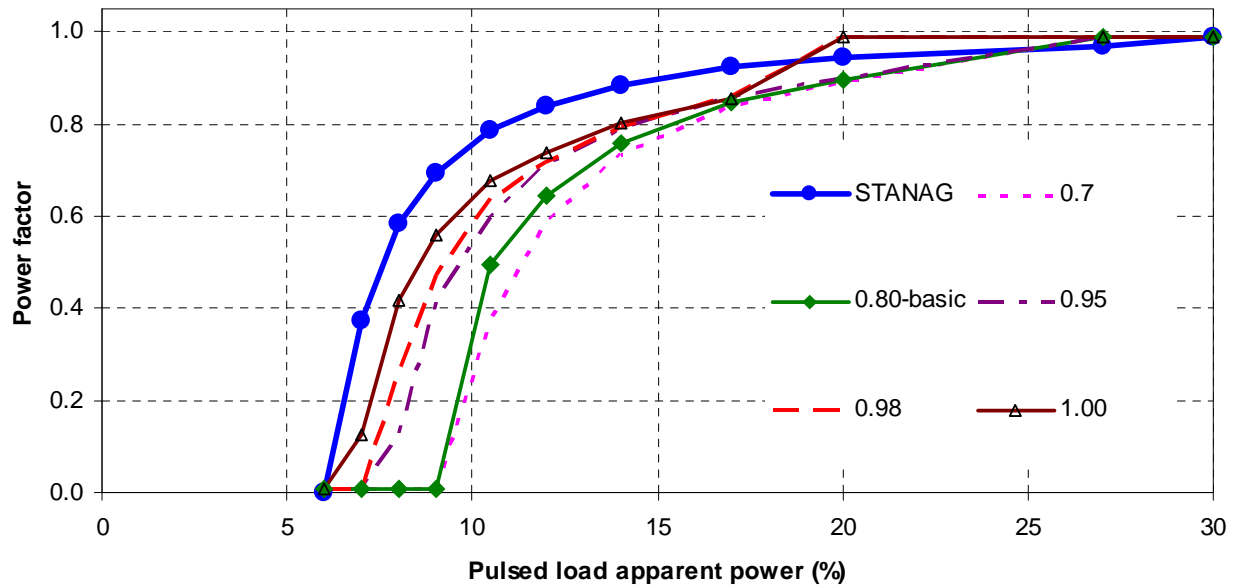
18

FIGURE 20. Power factor vs pulse load apparent power for different values of the service load power factor in the case of the conventional ship

High Voltage Cable's Equivalent Length

High voltage cable's equivalent length is a parameter, which is met only for the AES, because the typical conventional ship does not comprise high voltage network. In these case studies the system is simulated with high voltage cable's equivalent length of 50, 100, 150, 200, 250, 300, 350, 400 m.

For the case of the AES with the pulsed load installed at HV network, the respective power factor – pulsed load apparent power curves are extracted and presented in Fig. 21, which is properly enlarged in Fig. 22. It is obvious that the increase of high voltage cable's length tends to decrease slightly the unacceptable operating area.

For the case of the AES with the pulsed load installed at LV network, the respective power factor – pulsed load apparent power curves are extracted for different HV cable's equivalent length and they are presented in Fig. 23. Practically, these curves are the same, while there is a minor overlap of the unacceptable operating area determined by the STANAG 1008 curve from the one determined by the curves for pulsed load power factor higher than 0.80.

It is obvious that the HV cable's length is not a critical factor, especially for the AES with the pulsed load installed at LV network, because in this case voltage modulation is calculated at 440V.
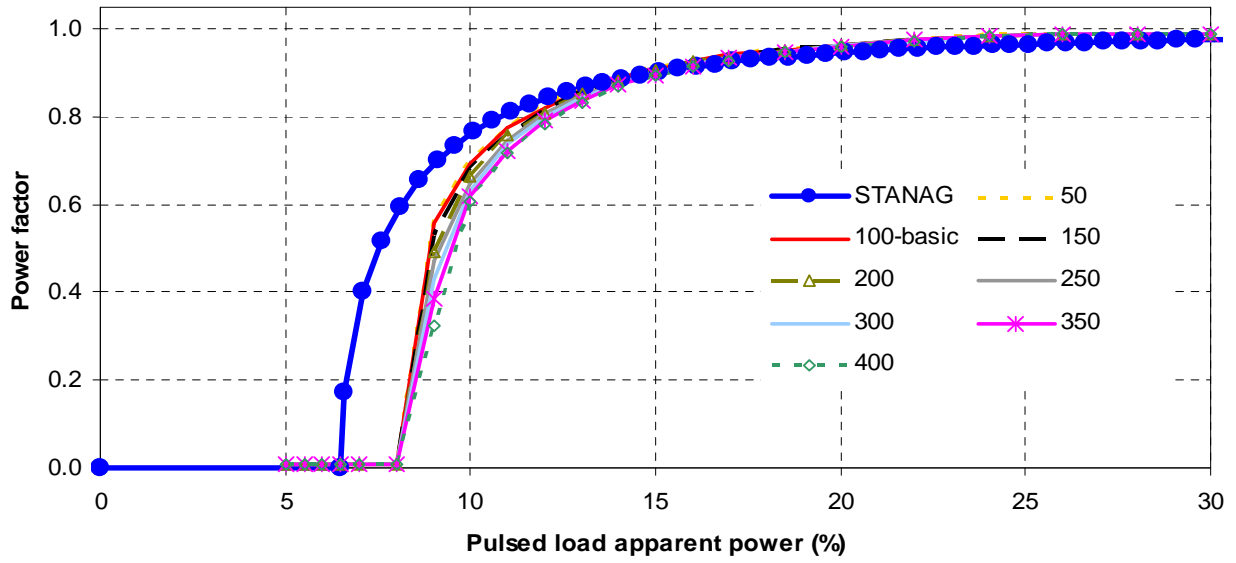
FIGURE 21. Power factor vs pulse load apparent power for different values of the HV cable's equivalent length in the case of the AES with pulsed load in HV network.
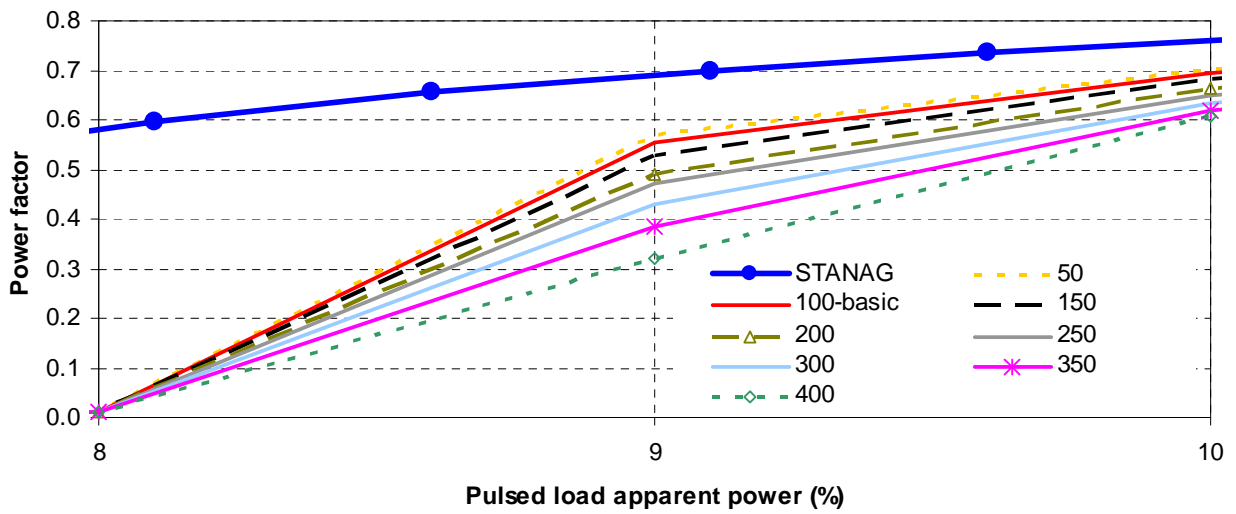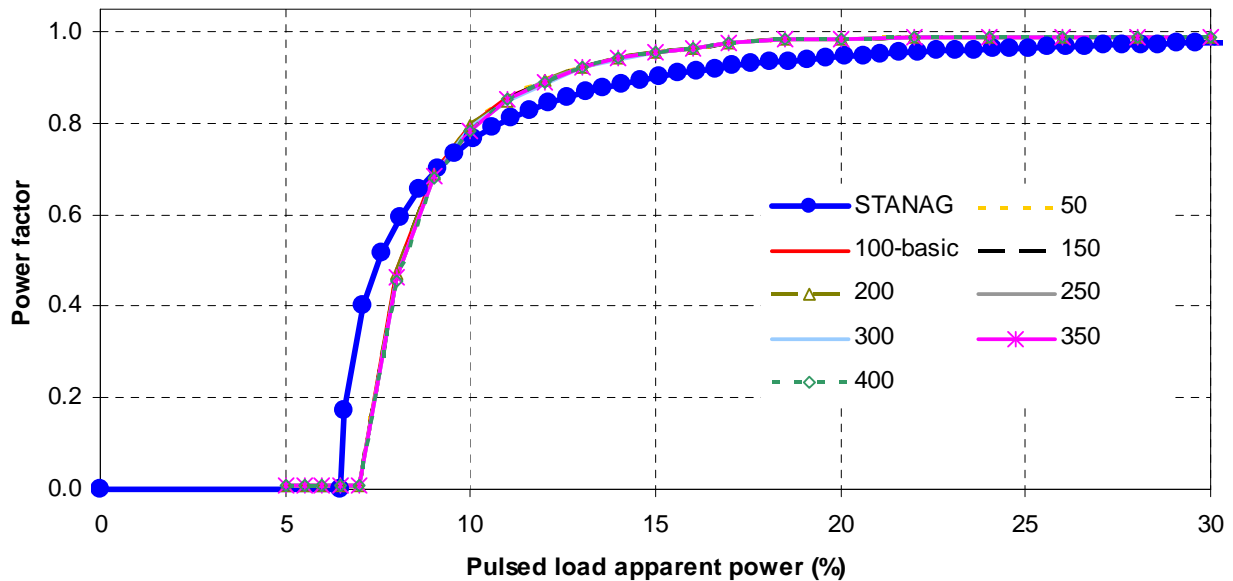

FIGURE 22. Enlargement of Fig. 21 with power factor vs pulse load apparent power for different values of the HV cable's equivalent length in the case of the AES with pulsed load in HV network.

FIGURE 23. Power factor vs pulse load apparent power for different values of the HV cable's equivalent length in the case of the AES with pulsed load in LV network.

440V Low Voltage Cable's Equivalent Length

In the following, the AES with the pulsed load in LV network is simulated repeatedly for different 440V voltage cable's equivalent length (50, 100 (basic scenario), 150, 200, 250, 300, 350, 400 m). The respective power factor – pulsed load apparent power curves are extracted, as it is shown in Fig. 24. It is obvious that the increase of the 440V low voltage cable's length tends to increase the unacceptable operating area. The respective curve of STANAG 1008 is proved quite insufficient as the cable's length and the pulsed load power factor increase.

For the case of the AES with the pulsed load installed at HV network, the respective power factor – pulsed load apparent power curves are extracted for different 440V LV cable's equivalent length and they are presented in Fig. 25. Practically, these curves are the same, while there is a minor overlap of the unacceptable operating area determined by the STANAG 1008 curve and the one from the curves obtained for pulsed load power factor higher than 0.90. This happens, because in this case the pulsed load is connected to the high voltage network and 440V LV cable's length has practically zero effect in the modulation phenomenon.

In case of the conventional ship, the respective power factor – pulsed load apparent power curves are extracted for different 440V LV cable's equivalent lengths (50, 150, 250, 400, 500 m) in Fig. 26. As the authors have already mentioned in [2], the increase of the 440V low voltage cable's length tends to increase the unacceptable operating area. The power factor – pulsed load apparent power curves are varied in an area wider than the ones of Fig. 24, which means that the respective effect is more significant in this case. This happens, because conventional ship's main load is connected to the 440V LV network, in contrast with the AES connected to the HV network.
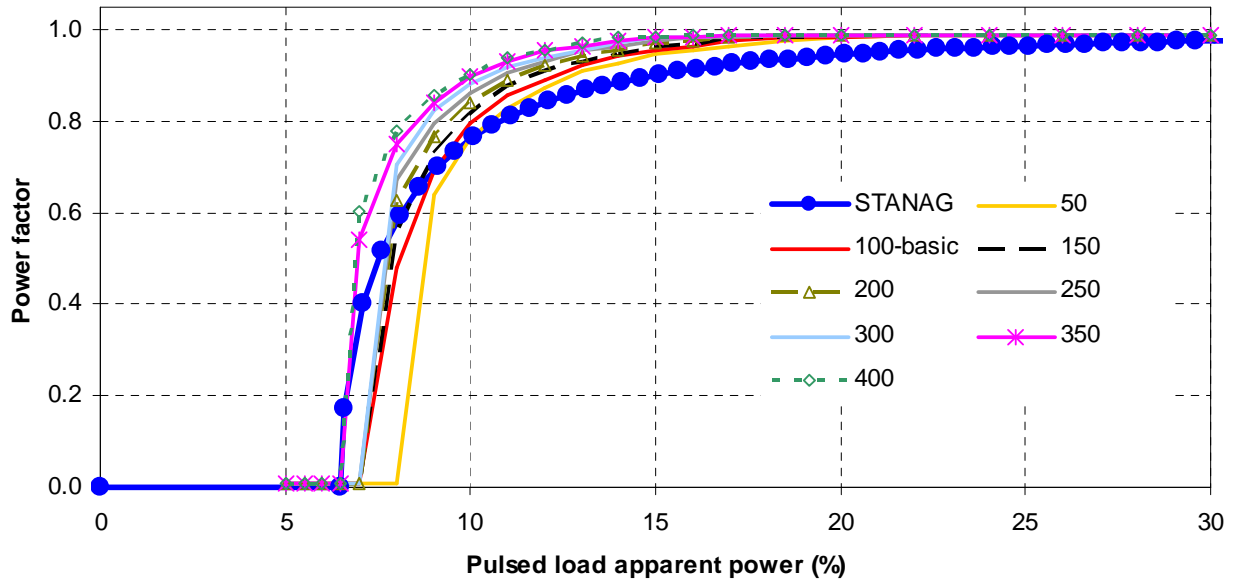
FIGURE 24. Power factor vs pulse load apparent power for different values of the 440V LV cable's equivalent length in the case of the AES with pulsed load in LV network.
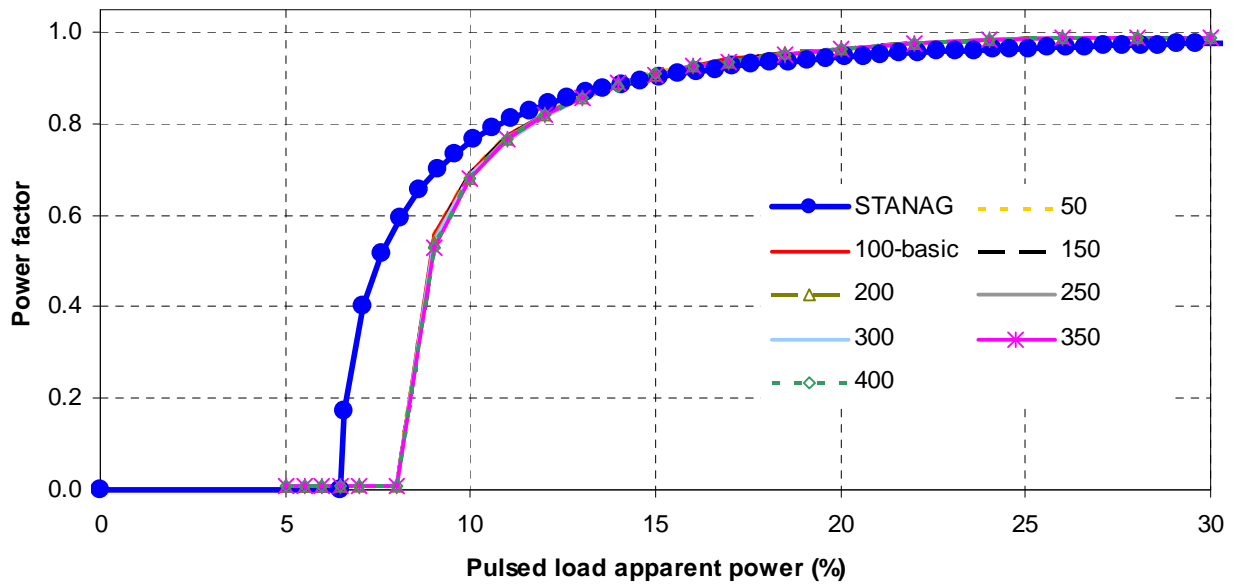

FIGURE 25. Power factor vs pulse load apparent power for different values of the 440V LV cable's equivalent length in the case of the AES with pulsed load in HV network.
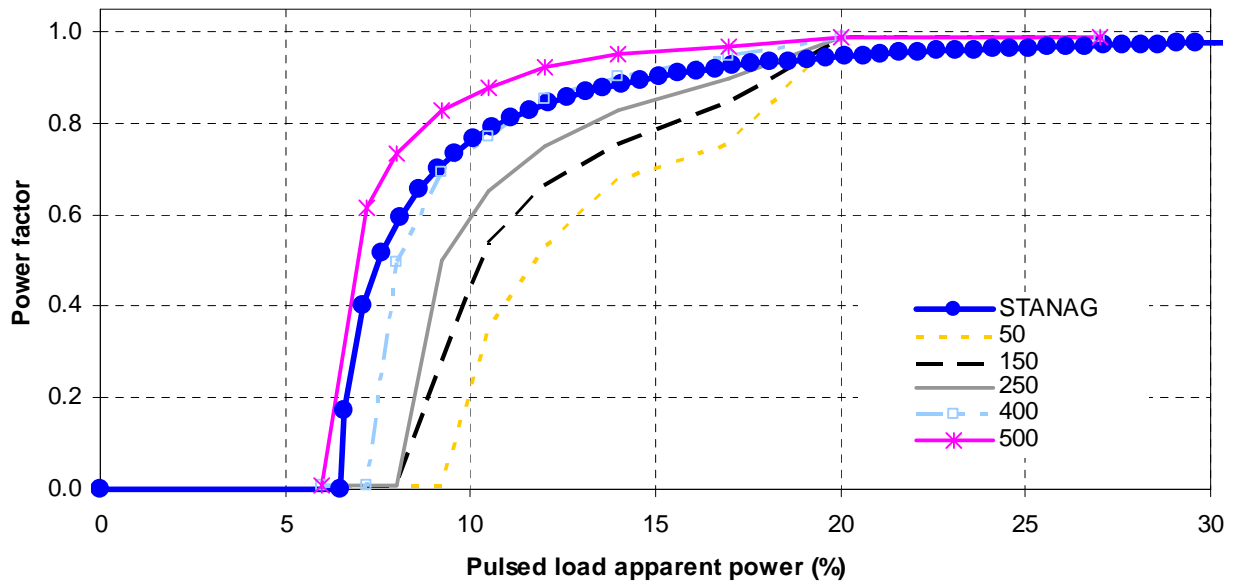
FIGURE 26. Power factor vs pulse load apparent power for different values of the 440V LV cable's equivalent length in the case of the conventional ship [2, Fig. 10] with the base load of the generator equal to 10%, pulsed load duty cycle 60% and pulsed load period 0.4 sec.

It is obvious that the 440V LV cable's length is a critical factor, except of the case of the AES with the pulsed load installed at HV network. In last one, the effect of the voltage modulation in the LV network is more limited. On the contrary, in cases of the conventional ship and the AES with the pulsed load installed at LV network it is observed that the longer the cables, the bigger the obtained unacceptable operating area.

115V Low Voltage Cable's Equivalent Length

In the following, the AES with the pulsed load in LV network is simulated repeatedly for different 115V low voltage cable's equivalent length (50, 100 (basic scenario), 150, 200, 250, 300, 350, 400 m). The respective power factor – pulsed load apparent power curves are extracted, as it is shown in Fig. 27. Practically, these curves are the same, while there is an overlap of the unacceptable operating area determined by the STANAG 1008 curve from the curves obtained for pulsed load power factor higher than 0.75.

For the case of the AES with the pulsed load installed at HV network, the respective power factor – pulsed load apparent power curves are extracted for different values of the 115V LV cable's equivalent length and they are presented in Fig. 28. Practically, these curves are the same, while there is a minor overlap of the unacceptable operating area determined by the STANAG 1008 curve from the curves obtained for pulsed load power factor higher than 0.90. Similar results are also obtained in case of the conventional ship

This happens, because the pulsed load is connected either to the high voltage network or to the 440V low voltage network, and 115V LV cable's length has practically zero effect in the modulation phenomenon.
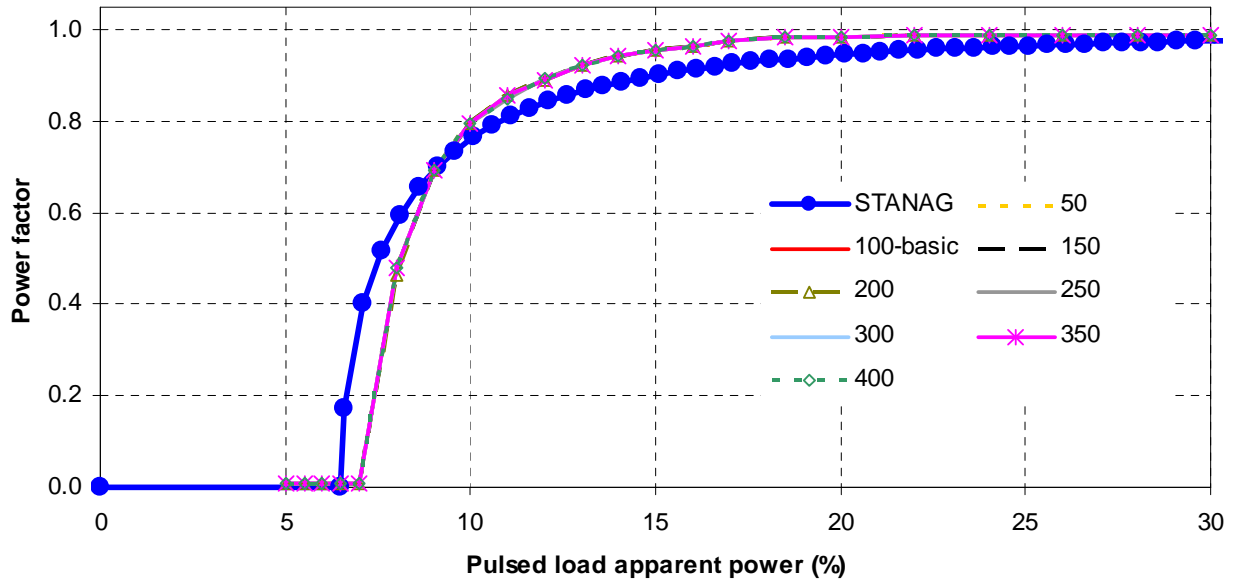
FIGURE 27. Power factor vs pulse load apparent power for different values of the 115V LV cable's equivalent length in the case of the AES with pulsed load in LV network.
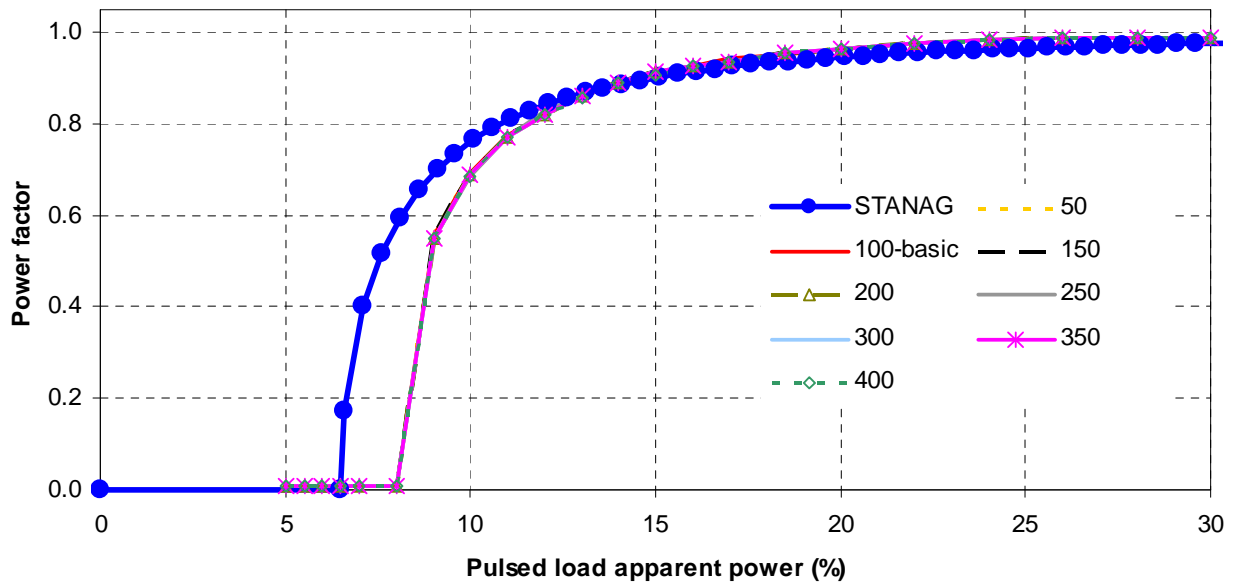

FIGURE 28. Power factor vs pulse load apparent power for different values of the 115V LV cable's equivalent length in the case of the AES with pulsed load in HV network.

Pulsed Load Period

Pulsed load period of should be greater than the power system period according to the STANAG 1008 request [2, § A.3.d].

In case of AES with the pulsed load installed at LV, the network is simulated repeatedly for different values of the pulsed load period (0.05 sec, 0.15 sec, 0.3 sec (basic scenario), 0.6 sec,

24

1.0 sec, 1.5 sec). The respective power factor – pulsed load apparent power curves are extracted, as it is shown in Fig. 29. It is obvious that the increase of the pulsed load period tends to increase the unacceptable operating area until the period reaches up to 1 sec. The respective curve of STANAG 1008 is proved quite insufficient for periods between 0.6 and 1.0 sec. It is mentioned that the simulation time is 2.5 sec except of the cases that period equals or is greater than 0.6 sec where the simulation duration is five times the respective period in order to permit the system reach "balanced" operation.
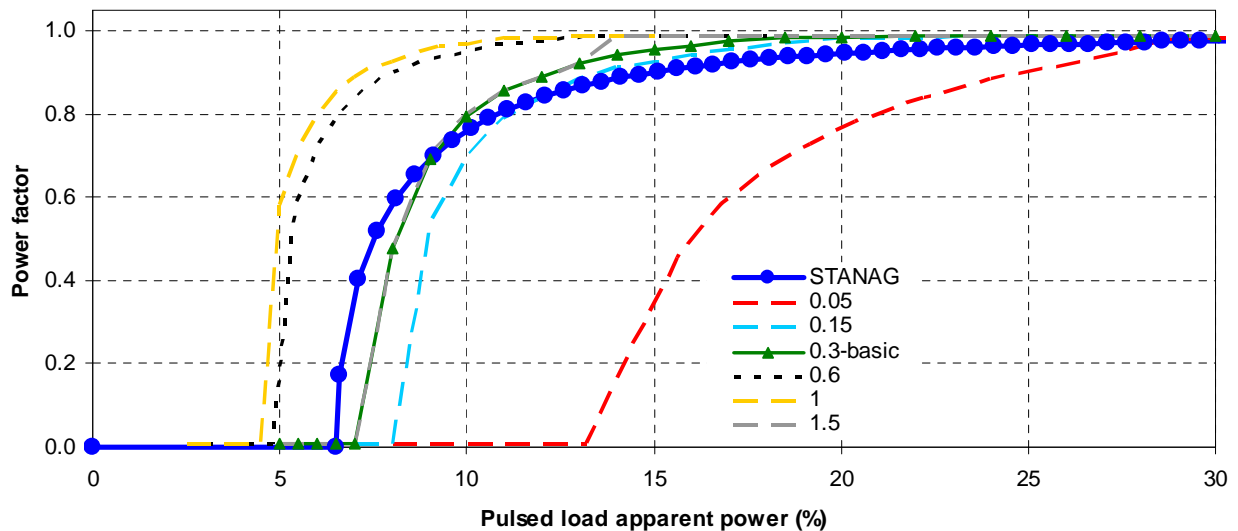

FIGURE 29. Power factor vs pulse load apparent power for different values of the pulsed load period in the case of the AES with pulsed load in LV network.

For the case of the AES with the pulsed load installed at HV network, the respective power factor – pulsed load apparent power curves are extracted for different values of the pulsed load period and they are presented in Fig. 30. Here, the increase of the pulsed load period tends to increase the unacceptable operating area until the period reaches up to 0.6 sec. For periods greater than 0.6 sec the respective area decreases (see curve with T=1 sec against T=0.6 sec). Especially, the curve with T=0.6 sec exceeds the unacceptable operating area determined by the STANAG 1008 curve. The power factor – pulsed load apparent power curves are located in an area wider than the previous ones of Fig. 29.

For the case of the conventional ship, as it is shown in Fig. 31, the increase of the pulsed load period tends to increase the unacceptable operating area until the period reaches up to 1.6 sec without exceeding the unacceptable operating area determined by the STANAG 1008 curve.

It is obvious that the pulsed load period is a critical factor affecting significantly the shape of the limitation curves and their position on the respective plane.
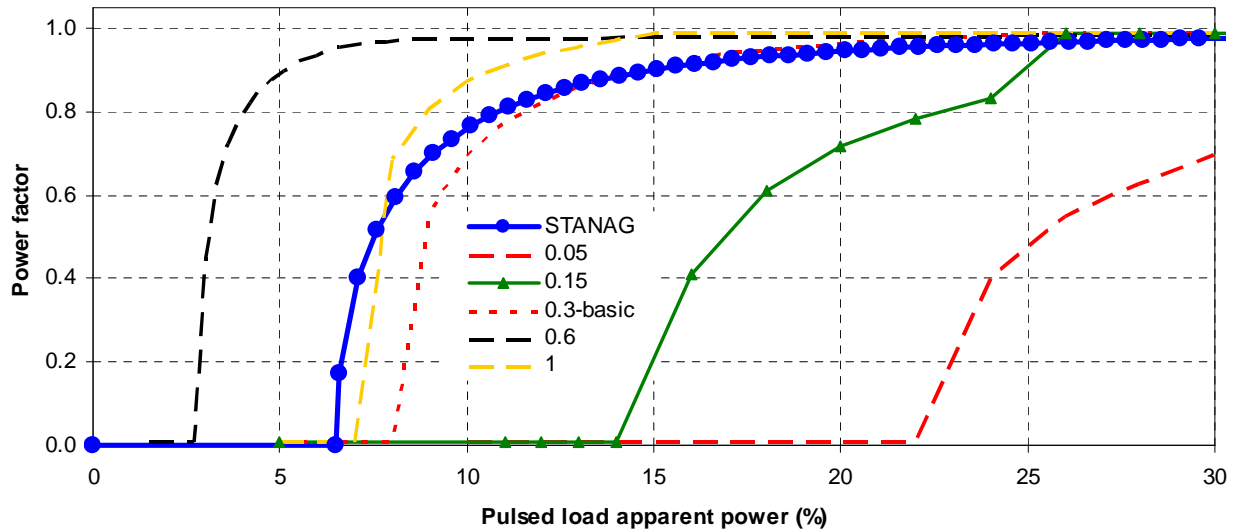
FIGURE 30. Power factor vs pulse load apparent power for different values of the pulsed load period in the case of the AES with pulsed load in HV network.
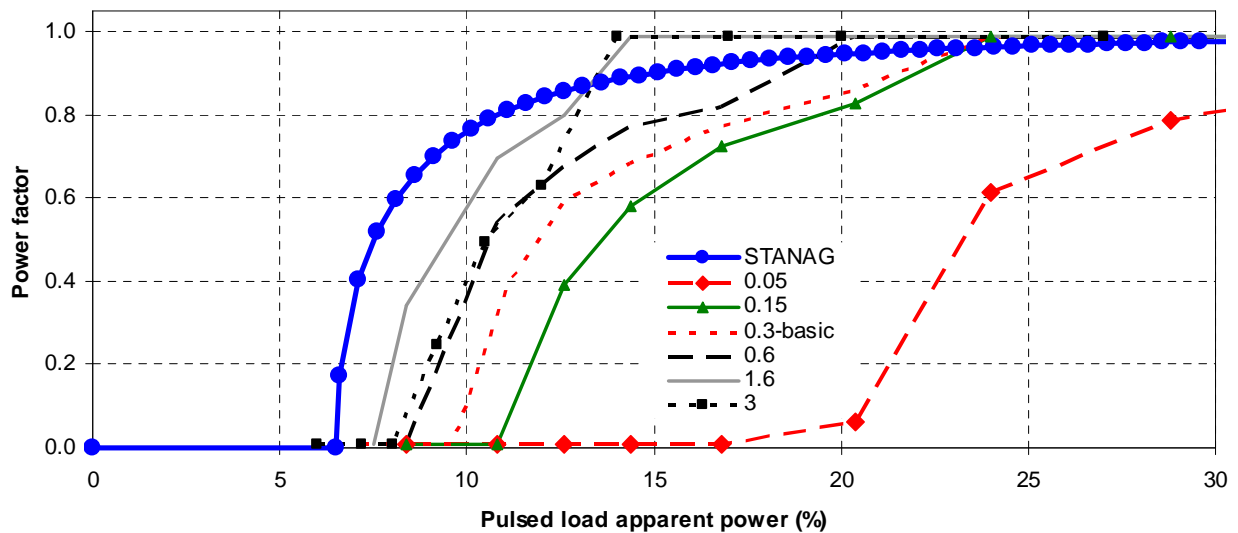

FIGURE 31. Power factor vs pulse load apparent power for different values of the pulsed load period in the case of the conventional ship [2, Fig. 11].

Pulsed Load Duty Cycle

Next, the AES with the pulsed load installed at LV, the network is simulated repeatedly for different pulsed load duty cycles (10%, 20%, 30%, 40%, 50% (basic scenario), 60%, 70%, 80%, 90%). In Fig. 32 the respective power factor – pulsed load apparent power curves are shown. The increase of the pulsed load duty cycle tends to increase the unacceptable operating area until the duty cycle reaches up to 70%. Increasing more of the duty cycle leads to the decrease of the respective area. STANAG 1008 curve seems to be slightly underestimated for duty cycles greater than 20% and for power factor higher than 0.7.
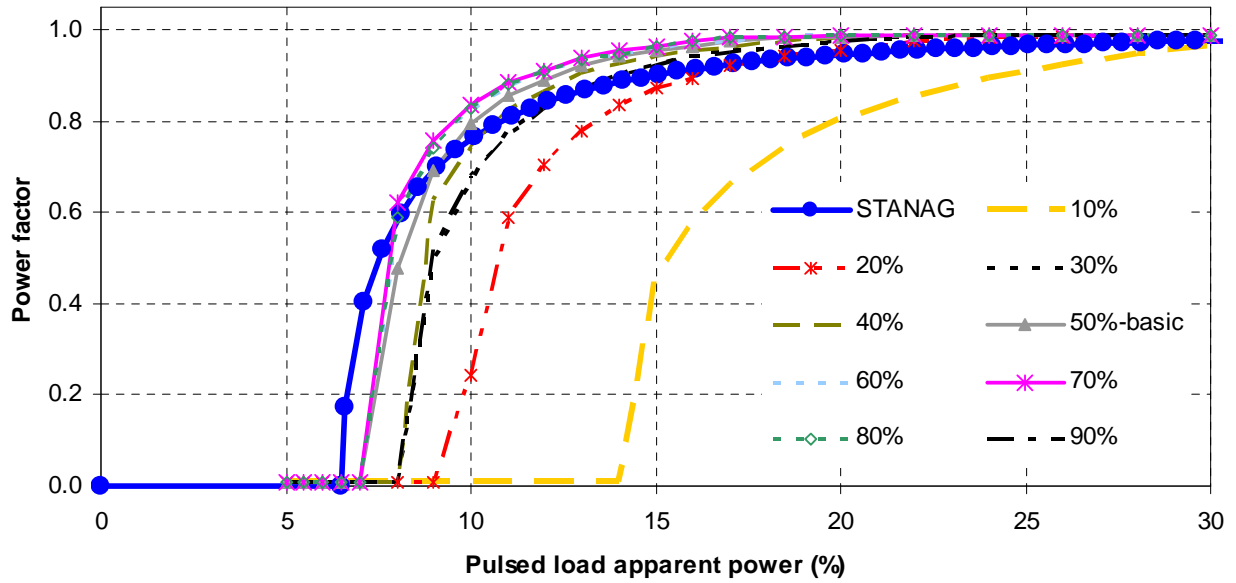
FIGURE 32. Power factor vs pulse load apparent power for different values of the pulsed load duty cycle in the case of the AES with pulsed load in LV network.

For the case of the AES with the pulsed load installed at HV network, the respective power factor – pulsed load apparent power curves are extracted for different values of the pulsed load duty cycle and they are presented in Fig. 33. Here, the increase of the pulsed load duty cycle tends to increase the unacceptable operating area until the duty cycle reaches up to 30%, while above 30% it tends to decrease the respective area. This means that the behavior of the power factor – pulsed load apparent power curves is different than the previous ones of Fig. 32.
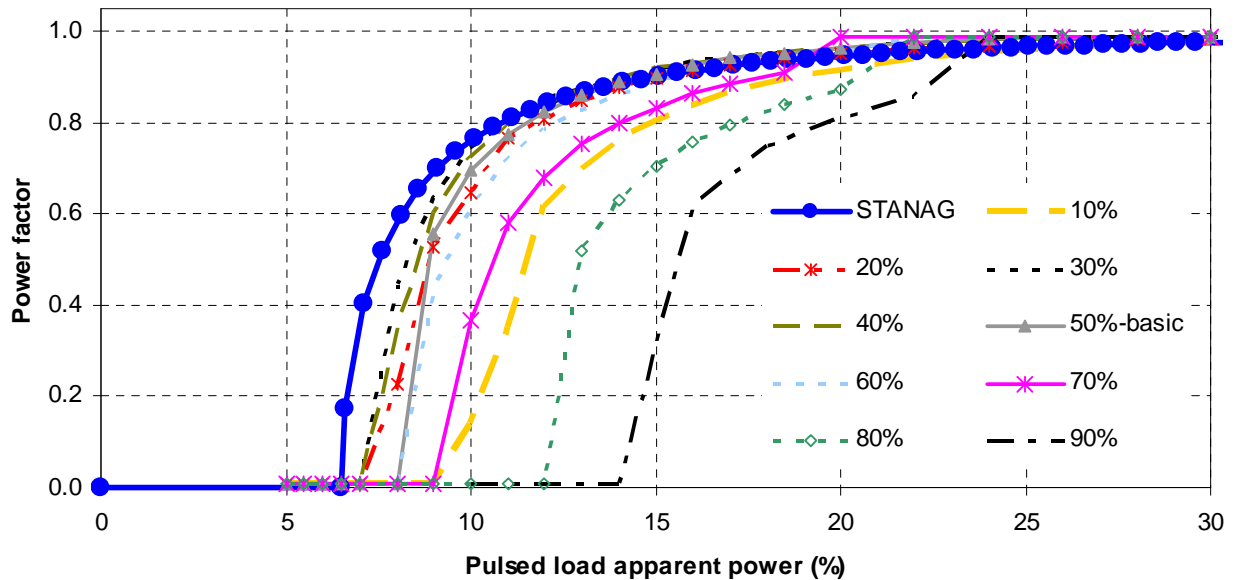

FIGURE 33. Power factor vs pulse load apparent power for different values of the pulsed load duty cycle in the case of the AES with pulsed load in HV network.
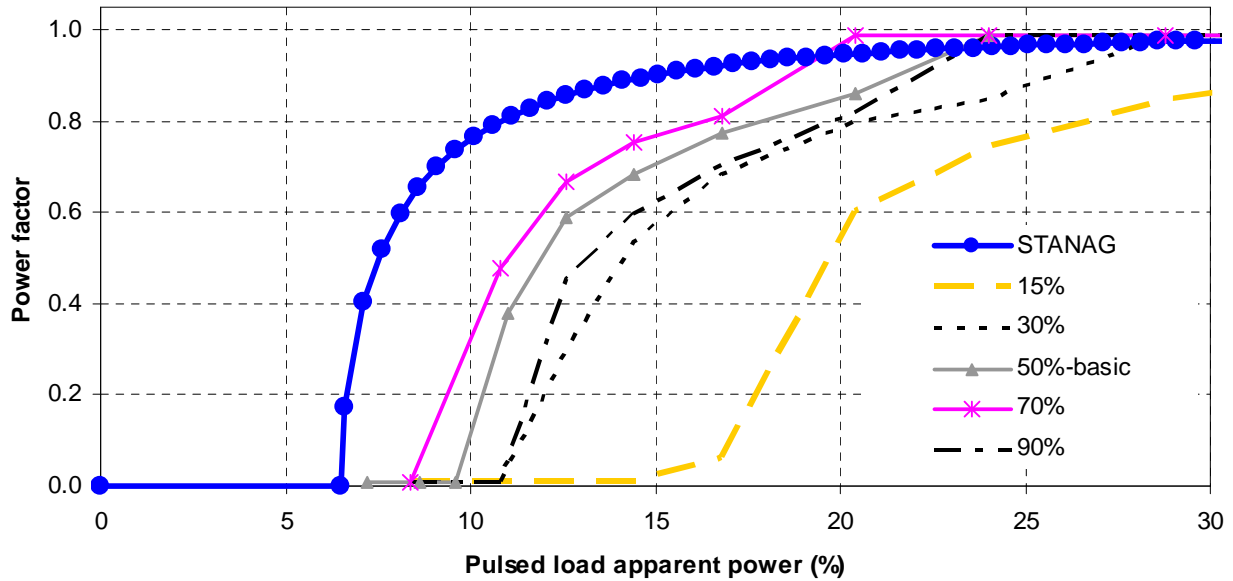
FIGURE 34. Power factor vs pulse load apparent power for different values of the pulsed load duty cycle in the case of the conventional ship [2, Fig. 12].

For the case of the conventional ship, as it is shown in Fig. 34, the increase of the pulsed load duty cycle tends to increase the unacceptable operating area until the duty cycle reaches up to 70%. Further increase leads to decrease of the respective area.

In the last two cases, there is a minor overlap of the unacceptable operating area determined by the STANAG 1008 curve from the curves obtained for a 70%duty cycle.

Pulsed load duty cycle is a significant parameter, which determines affects significantly the unacceptable operating area on the power factor – pulsed load apparent power plane.

Generator's Sub-transient Reactance

In the following, the AES with the pulsed load installed at LV network is simulated repeatedly for different values of the generator's sub-transient reactance of d-axis $X_d^{//}$ (12,5%, 15% (basic scenario), 17.5%, 20%, 25%, 30%). Simultaneously, it is considered that the respective sub-transient reactance of q-axis $X_q^{//}$ equals to $X_d^{//}$. In Fig. 35 the respective power factor – pulsed load apparent power curves are shown. It is obvious that for very small values of $X_d^{//}$ the unacceptable operating area is increased (see curve of 12.5%), while practically the curves of 15% and 30% are identical, as well as the curves of 17.5%, 20% and 25%. The respective STANAG curve approaches the respective curves sufficiently, except the curve obtained for $X_d^{//} = X_q^{//} = 12,5\%$.

In Fig. 36 the respective power factor – pulsed load apparent power curves are extracted for different values of $X_d^{//}$ (15%, 17.5%, 20%, 25%, 30%) and for the AES with the pulsed load installed at HV network. The respective results are similar with the previous ones, even if the respective curves are spread in a wider area than the previous one of Fig. 35.

Regarding the case of the conventional ship, as the authors have already mentioned in [2] and as it is shown in Fig. 37, the unacceptable operating area of the respective STANAG 1008 curve contains the respective areas of the estimated curves.

The obtained results demonstrate that the generator's sub-transient reactance affects considerably the unacceptable operating area, especially for small values of $X_d^{//}$. This leads to

the conclusion that it is one of the parameters that must be considered for the design of the respective power system.
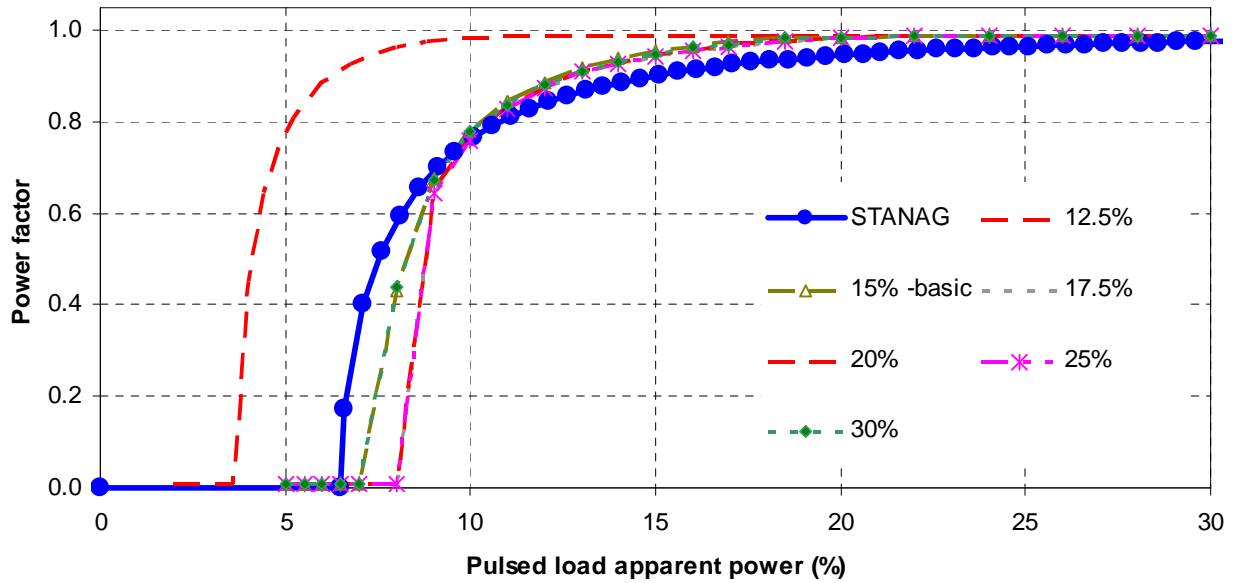

FIGURE 35. Power factor vs pulse load apparent power for different values of the generator's sub-transient reactance in the case of the AES with pulsed load in LV network.
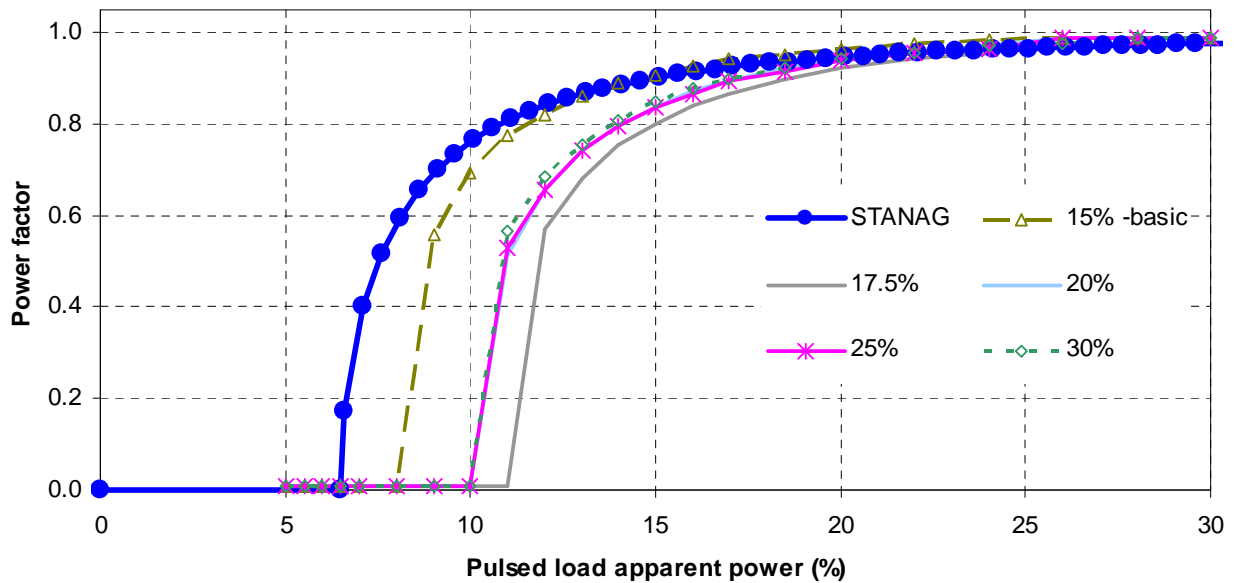

FIGURE 36. Power factor vs pulse load apparent power for different values of the generator's sub-transient reactance in the case of the AES with pulsed load in HV network.
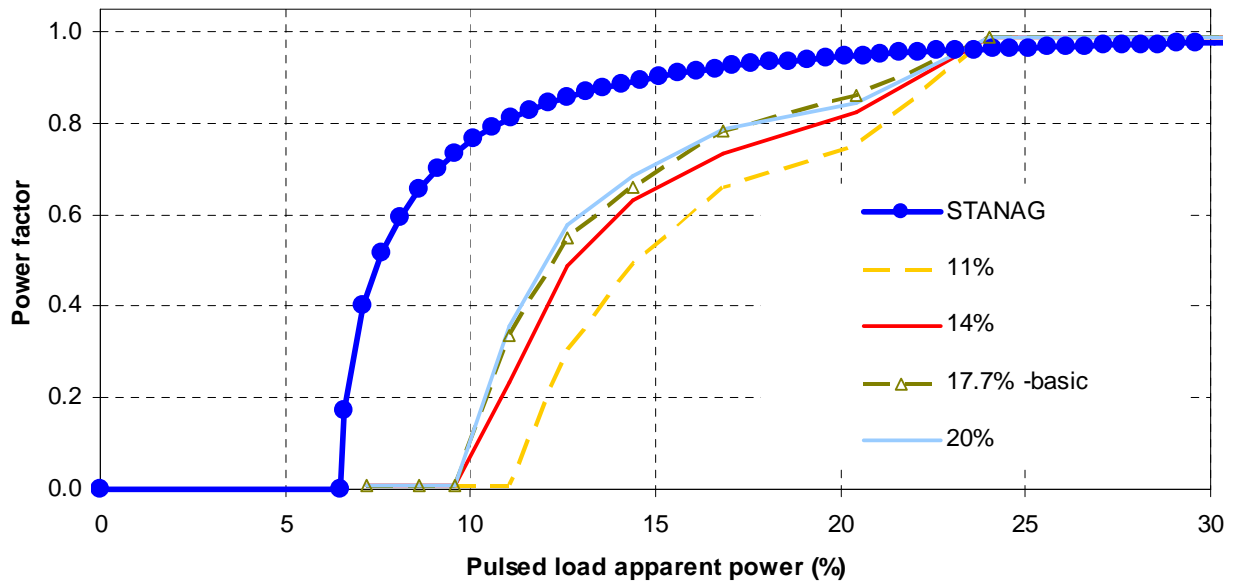
FIGURE 37. Power factor vs pulse load apparent power for different values of the generator's sub-transient reactance in the case of the conventional ship [2, Fig. 8].

Generator's Inertia

Next, the AES with the pulsed load installed at LV network is simulated repeatedly for different values of the generator's inertia (1.00, 1.25, 1.5 (basic scenario), 1.75, 2.00, 2.50, 3.00). In Fig. 38 the respective power factor – pulsed load apparent power curves are shown, where no significant effect is observed for this range of values.
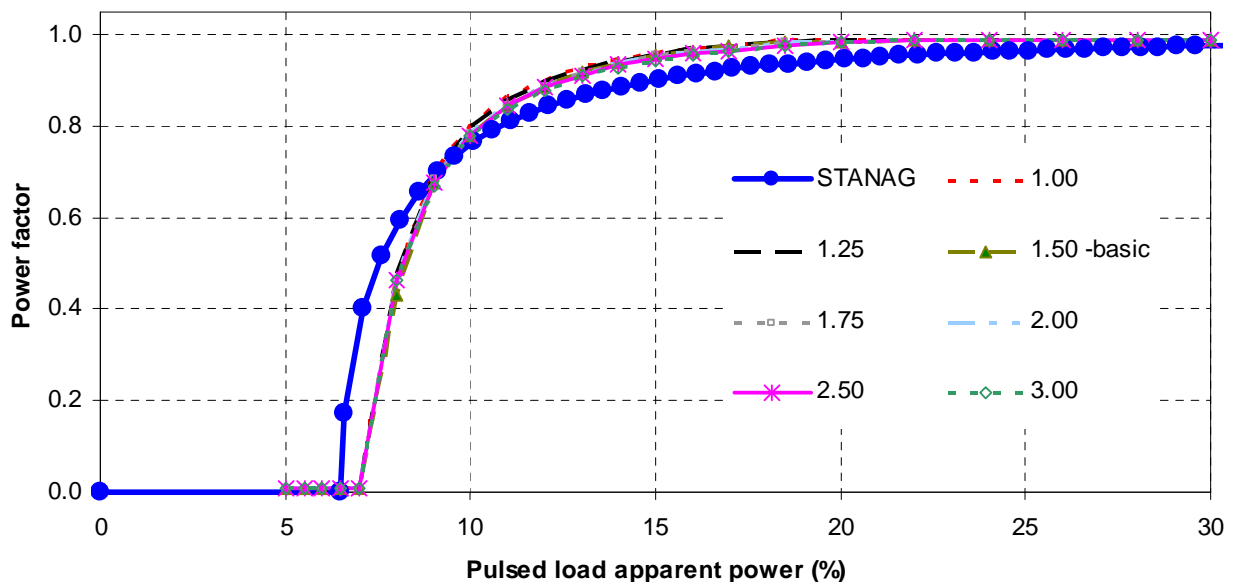

FIGURE 38. Power factor vs pulse load apparent power for different values of the generator's inertia in the case of the AES with pulsed load in LV network.

Similarly, in Fig. 39 the respective power factor – pulsed load apparent power curves are shown for different values of inertia (0.75, 1.00, 1.25, 1.5 (basic scenario), 1.75, 2.00, 2.50, 3.00) and obtained for the AES with the pulsed load installed at HV network. The respective results are similar with the previous ones, even if the respective curves are slightly different for small apparent power of pulsed load. In case of the conventional ship, as it has already mentioned in [2] and as it is shown in Fig. 40, no significant effect is observed on the respective. Only for power factor larger than 0.8 and small generator inertia values the curves begin to separate.
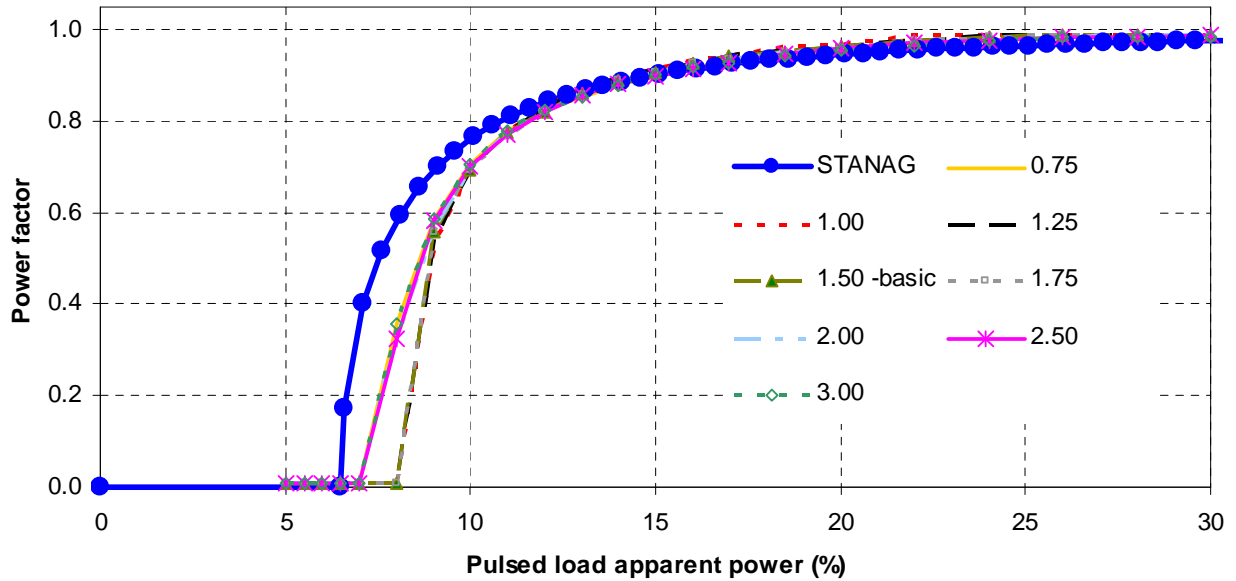

FIGURE 39. Power factor vs pulse load apparent power for different values of the generator's inertia in the case of the AES with pulsed load in HV network.
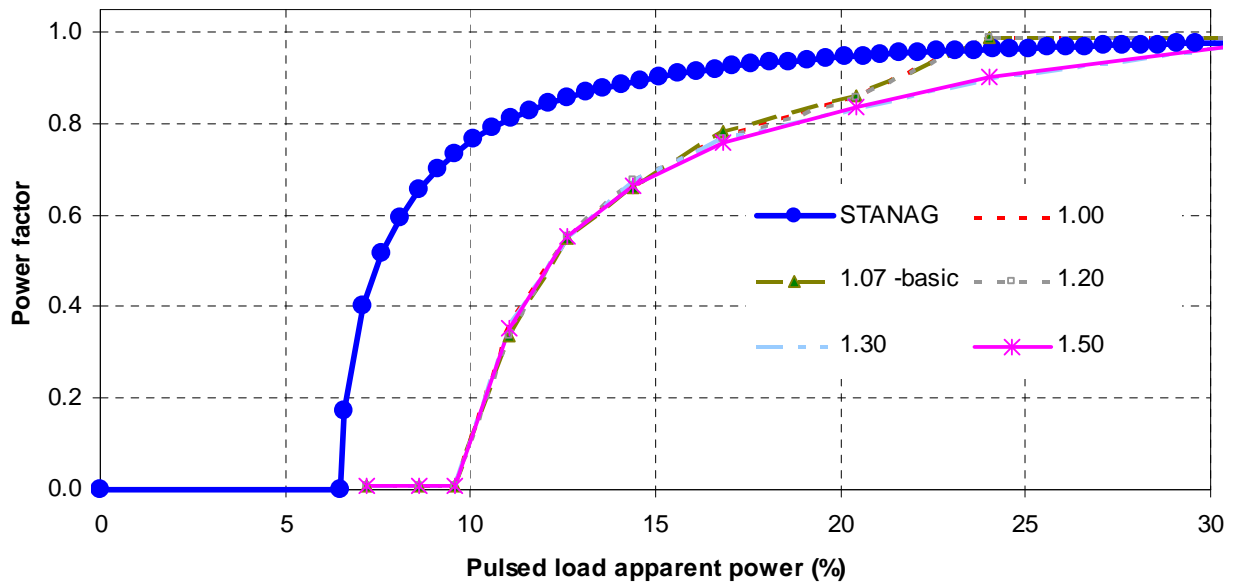

FIGURE 40. Power factor vs pulse load apparent power for different values of the generator's inertia in the case of the conventional ship [2, Fig.9].

31

A long series of simulation results not provided here due to space limitations also led to the conclusion that average frequency modulation decreases with inertia constant increase. This is expected as the bigger the generator inertia the lower the speed variations due to load changes. As it was shown above, generator inertia affects slightly the unacceptable operating area.

Governor's Gain

Next, an AES with the pulsed load installed at LV network is simulated repeatedly for different values of the governor's gain K (10, 20, 30, 40 (basic scenario),50, 60). In Fig. 41 the respective power factor – pulsed load apparent power curves are shown, where no significant effect is observed for this range of values. Similarly, the respective power factor – pulsed load apparent power curves for different values of governor's gain for the AES and the pulsed load installed at HV network are shown in Fig. 42. They resemble to the previous ones. In case of the conventional ship, as it has already mentioned in [2] and as it is shown in Fig. 43, no significant effect is observed on the respective curves, except from operation with power factors larger than 0.75, where curves begin to separate.

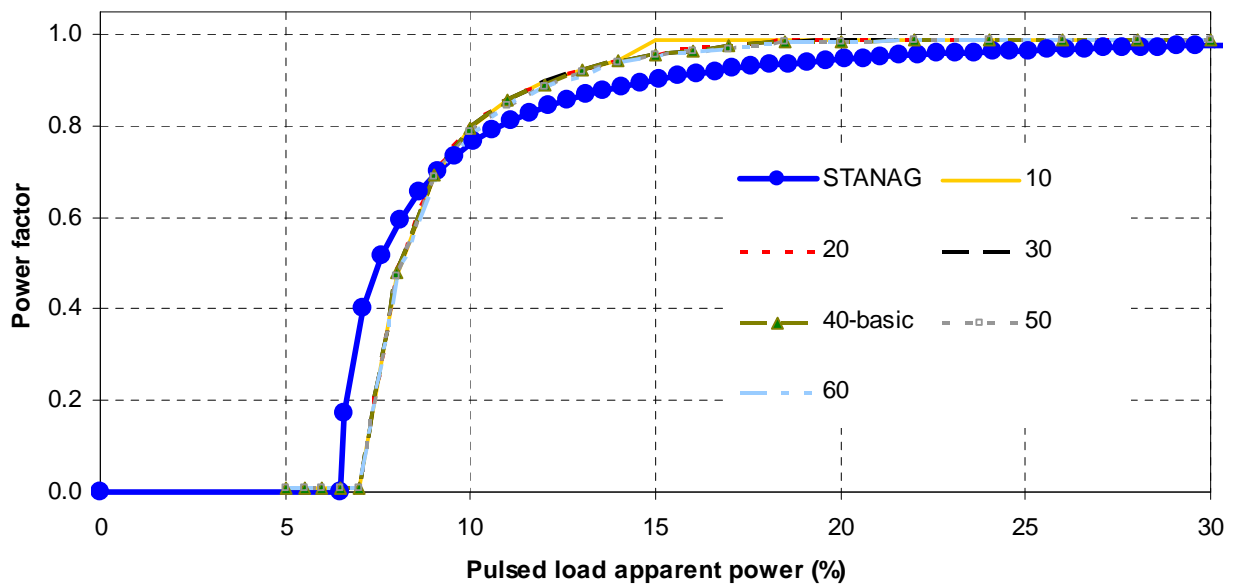Finally, it is concluded that the governor's gain has a weak effect on the unacceptable operating area.

FIGURE 41. Power factor vs pulse load apparent power for different values of the governor's gain in the case of the AES with pulsed load in LV network.
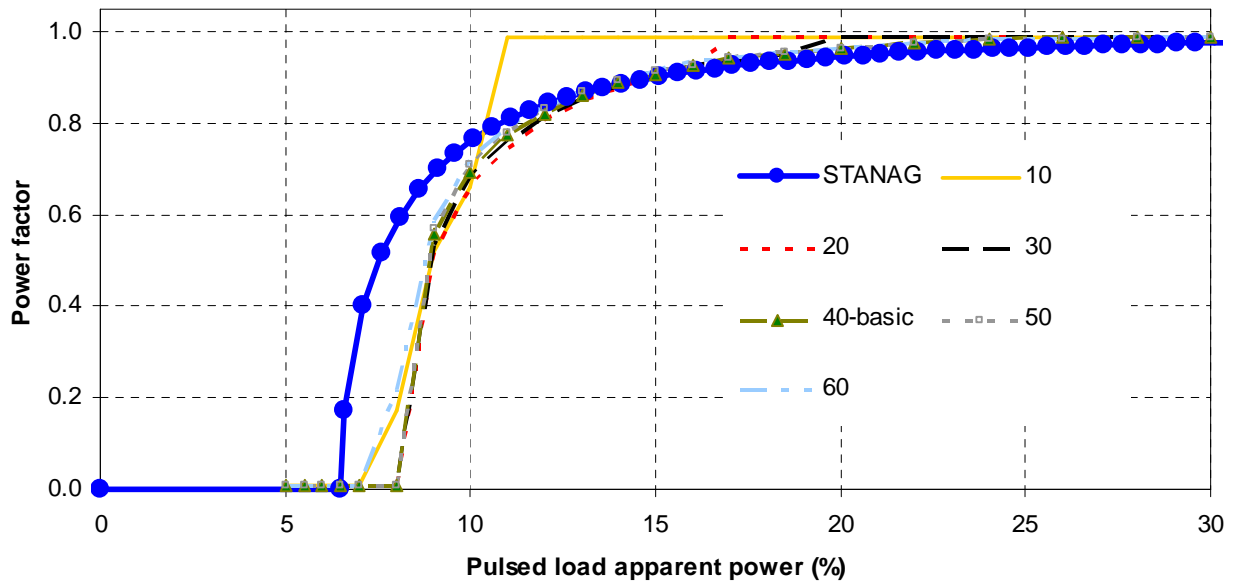
FIGURE 42. Power factor vs pulse load apparent power for different values of the governor's gain in the case of the AES with pulsed load in HV network.

FIGURE 43. Power factor vs pulse load apparent power for different values of the governor's gain in the case of the conventional ship [2].

AVR Gain

Next, the AES with the pulsed load installed at LV network is simulated repeatedly for different values of the AVR gain K_A (50, 100 (basic scenario), 150, 200, 250). The respective power factor – pulsed load apparent power curves are shown in Fig. 44, where it is obvious that the increase of the AVR gain tends to extend the unacceptable operating area, outside the area defined by STANAG 1008 curve.

Similarly, in Fig. 45 the respective power factor – pulsed load apparent power curves are shown for different values of AVR gain K_A (50, 100, 150, 200 (basic scenario), 225) and for the AES with the pulsed load installed at HV network. Here, the increase of the AVR gain tends to increase the unacceptable operating area, but not beyond the limitation curve defined by STANAG 1008. Larger values for AVR gain can not be provided as system is led to instability.

In case of the conventional ship, no significant effect is observed on the respective curves as it has already mentioned in [2] and as it is shown in Fig. 46.

FIGURE 44. Power factor vs pulse load apparent power for different values of the AVR gain in the case of the AES with pulsed load in LV network.

FIGURE 45. Power factor vs pulse load apparent power for different values of the AVR gain in the case of the AES with pulsed load in HV network.
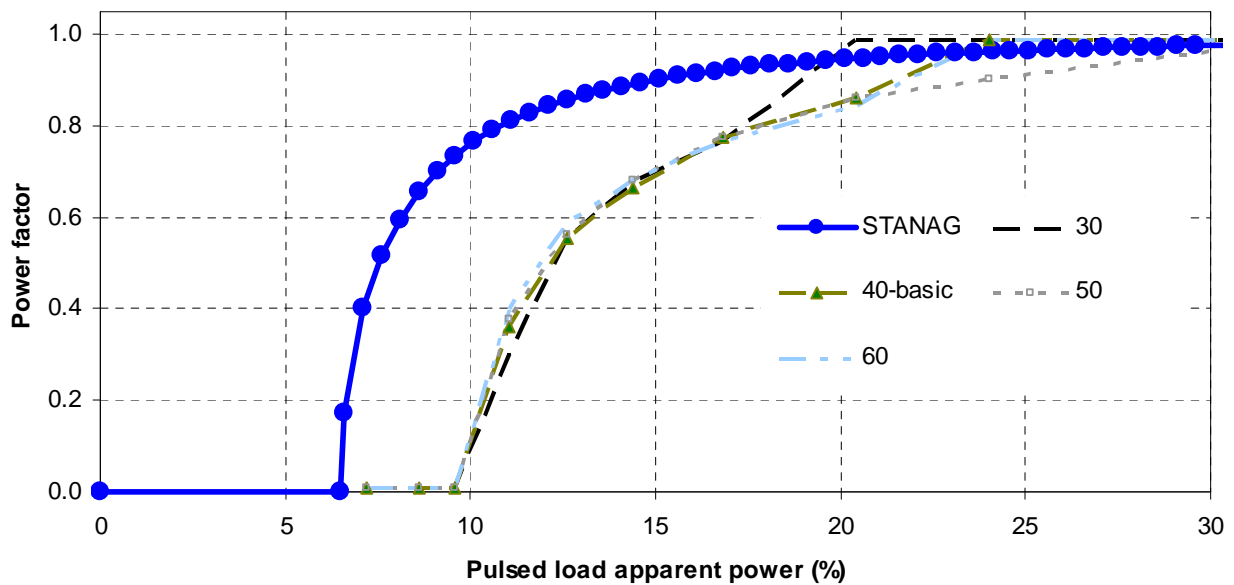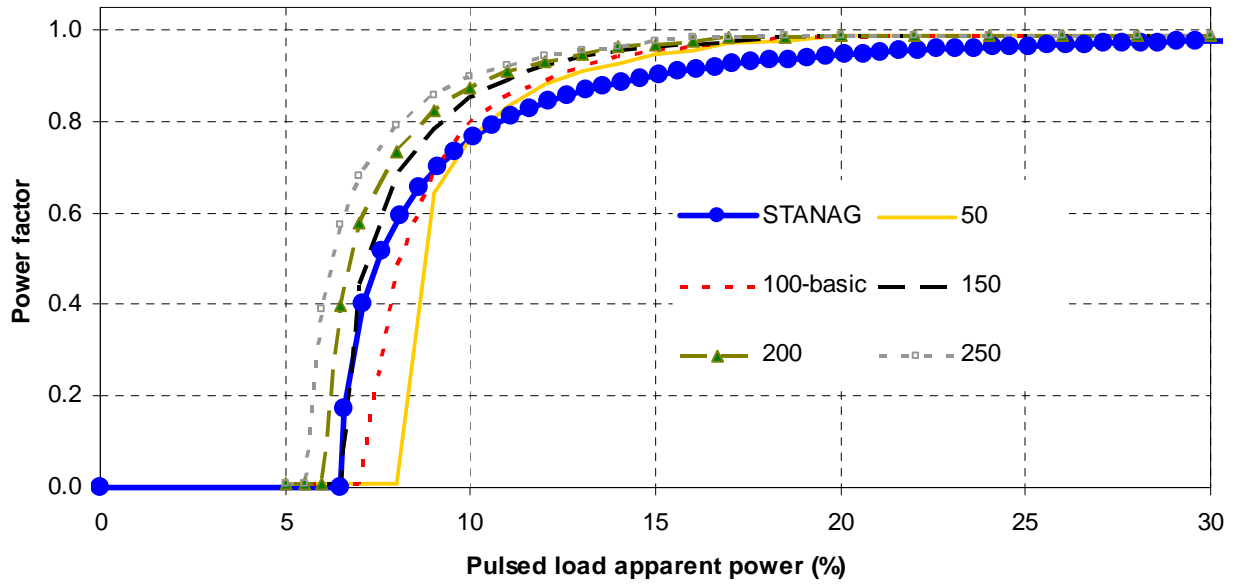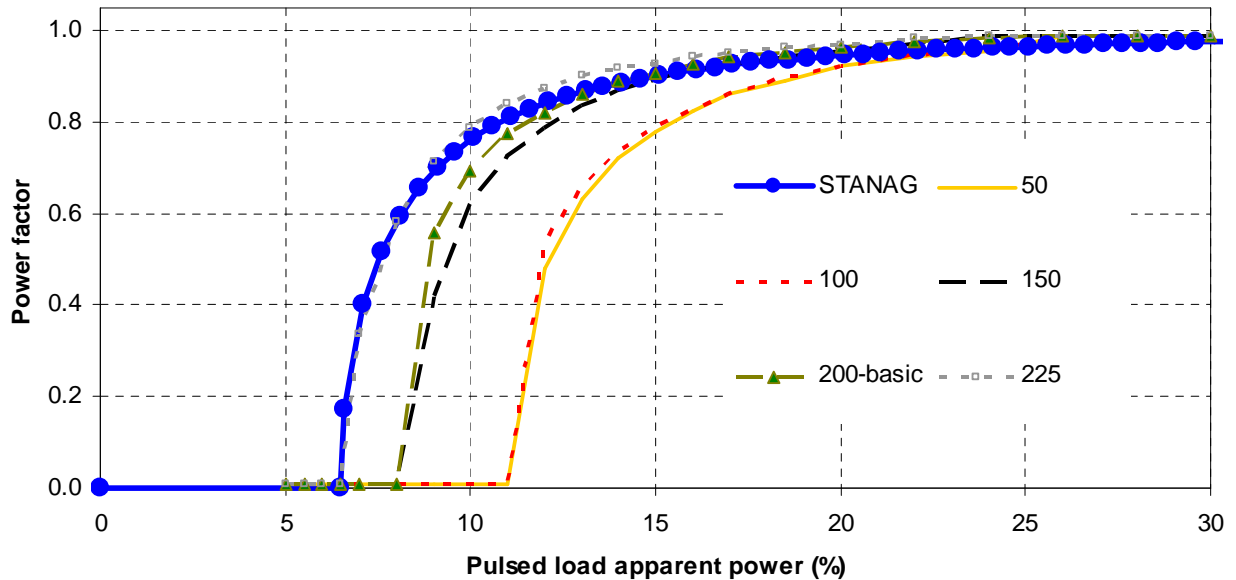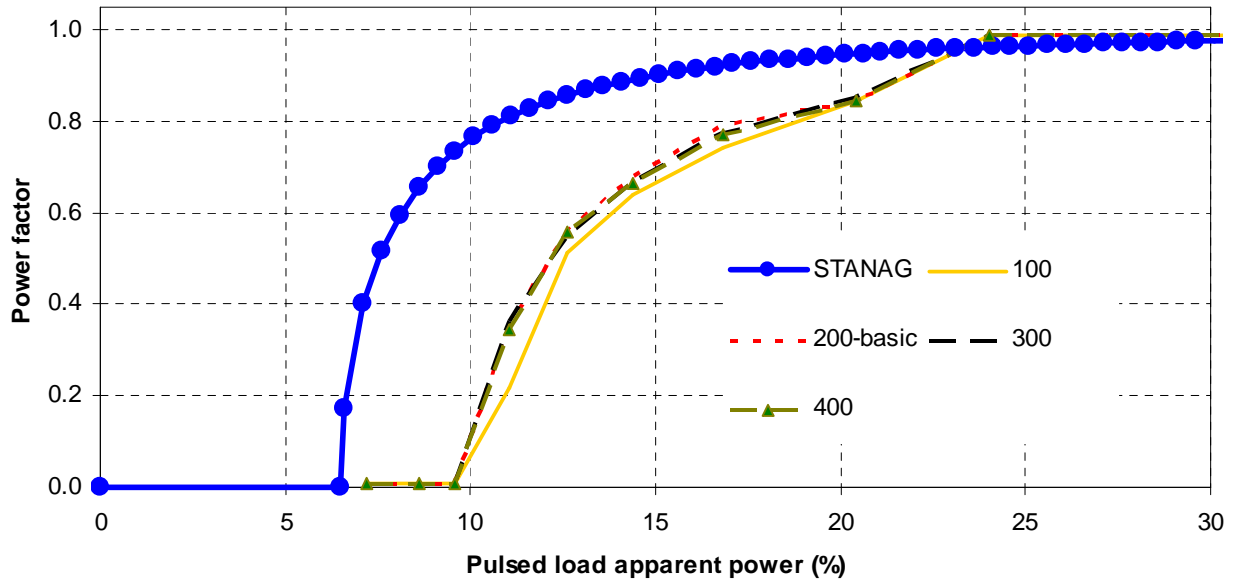
34

FIGURE 46. Power factor vs pulse load apparent power for different values of the AVR gain in the case of the conventional ship [2].

It is concluded that the AVR gain has strong effect on the obtained unacceptable operating area for the AES topologies.

Generator's Field Voltage Upper Bound

Next, the AES with the pulsed load installed at LV network is simulated repeatedly for different values of the generator's field voltage upper bound, V_{Rmax} (1.25, 2, 4, 6 (basic scenario),8, 10, 12). In Fig. 47 the respective power factor – pulsed load apparent power curves are shown. The curves obtained for V_{Rmax}=4, 6, 8, 10, 12 are identical. It is obvious that the respective parameter tends to increase the unacceptable operating area for very small values (less than 2). However, the usual values are above 3.

Similarly, the respective power factor – pulsed load apparent power curves for different values of the generator's field voltage upper bound V_{Rmax} and for the AES with the pulsed load installed at HV network are shown in Fig. 48. Here, the curves present the same behavior with the ones of the AES with the pulsed load connected to LV network, but with larger range of variation. In case of the conventional ship no significant effect is observed on the respective curves.

The results presented above demonstrate that generator's field voltage upper bound has weak effect on the unacceptable operating area for typical values (equal or greater than 3.0).

35
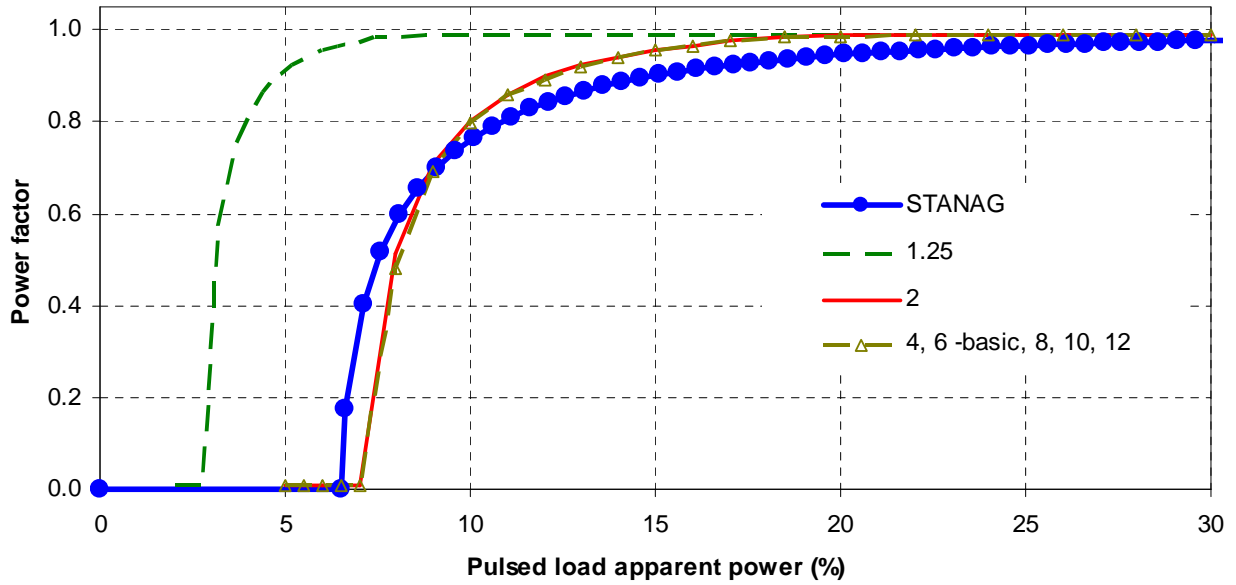
FIGURE 47. Power factor vs pulse load apparent power for different values of the bound of the generator's field voltage in the case of the AES with pulsed load in LV network.
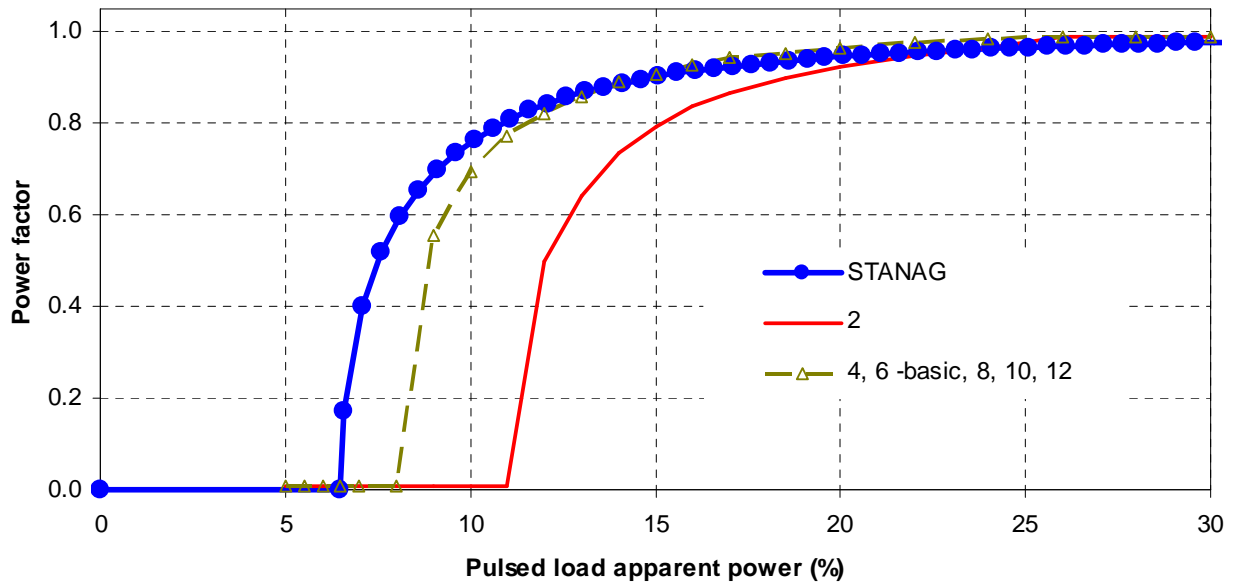
FIGURE 48. Power factor vs pulse load apparent power for different values of the bound of the generator's field voltage in the case of the AES with pulsed load in HV network.

CONCLUSIONS

In this paper the STANAG 1008 design constraints for voltage / frequency modulation have been examined extending its application from the conventional ships to the AES. The last one includes high voltage electric power generation, low voltage ship service power supply system,

high voltage electric propulsion, high or low voltage pulsed loads, while the conventional ship only low voltage network.

Voltage and frequency modulation measure at low voltage sub-networks is studied via simulations in Matlab / Simulink, taking into account various parameters affecting the entire phenomenon. The significance of the respective effects are presented synoptically in Table 4 for three different topologies examined:

- conventional ship electrical network,
- AES with pulsed load installed at low voltage system,
- AES with pulsed load installed a high voltage system.

TABLE (4). Gravity of the effects of various parameters in the voltage/ frequency modulation for each ship topology.

Ship power system Parameter	Conventional	AES with pulsed load in LV network Gravity	AES with pulsed load in HV network
Service load factor of the generator at the time of the pulsed load occurrence	Significant	Very significant	Very significant
Ratio of HV service load apparent power to the total apparent power	- (no existence)	Less significant	Less significant
Ratio of 440V service load apparent power to the total apparent power	Less significant	Less significant	Less significant
Ratio of 115V service load apparent power to the total apparent power	Less significant	No significant	No significant
Service load power factor	Very significant	Very significant	Very significant
HV cable equivalent length	- (no existence)	No significant	Less significant
440V cable equivalent length	Significant	Less significant	No significant
115V cable equivalent length	Very significant	No significant	No significant
Pulsed load period	Very significant	Very significant	Very significant
Pulsed load duty cycle	Very significant	Very significant	Very significant
Generator's sub-transient reactance	Significant	Significant	Significant
Generator's inertia	Less significant	No significant	Less significant
Governor's gain	No significant	No significant	No significant
AVR gain	Less significant	Significant	Significant
Bound of generator's field voltage	Less significant	Less significant	Less significant

In more detail, the effect of each studied parameter is analyzed next:

- Service load factor of the generator at the time of the pulsed load occurrence the presents a strong effect, especially in the case of AES. The variation of this factor beyond 0.20 tends to increase significantly the unacceptable operating area. In this case the design constraints of STANAG 1008 are proved to be insufficient.
- In case of service load distribution to different voltage networks the analysis of the obtained results is more complicated. The ratio of the rated apparent power of the voltage network that the pulsed load is connected to, to the total service load apparent power has a weak effect while the rest of the ratios do not practically affect.
- The effect the service load power factor is very significant, especially in case of the AES. The variation of this factor out of the range of 0.70 - 0.80 tends to increase the unacceptable operating area and the design constraints of STANAG 1008 are insufficient.
- The effect equivalent length of the cables connecting the generator and the pulsed load is less significant. The rest of the cables' lengths do not practically affect. In the case of the AES with the pulsed load installed at high voltage network the increase of the high

voltage cable's equivalent length tends to decrease slightly the unacceptable operating area. In case of the AES with the pulsed load installed at 440V low voltage network or the conventional ship the increase of the 440V low voltage cable's equivalent length tends to increase significantly the unacceptable operating area.

- Pulsed load period the effect is very significant. Maintaining it within 0.6 – 1.0 sec any increase tends to increase the unacceptable operating area while any further increase leads to decrease the unacceptable operating area. Generally, the design constraints of STANAG 1008 are proved insufficient in this case.
- Pulsed load duty cycle is a very significant parameter. Any increase of this factor until 70% (for the cases of the conventional ship and of AES with the pulsed load installed at LV network) or 30% (for the case of AES with the pulsed load installed at HV network) tends to increase the unacceptable operating area, while further increase is decreasing the area. The design constraints of STANAG 1008 are proved insufficient in case of AES.
- Generator's sub-transient reactance is a very significant parameter lacking of a regular behavior. In case of AES, the design constraints of STANAG 1008 are insufficient for very small values of generator's sub-transient reactance.
- Generator's inertia the effect is less significant for very small values of this parameter, while for larger values do not present any effect.
- Governor's gain there has no effect for the typical values. Only for very small values or very big values (such as 10 and 60) a small shift of the curves occurs.
- Automatic Voltage Regulator (AVR) gain effect is significant, especially in the case of the AES. The increase of this factor tends to increase the unacceptable operating area, while the design constraints of STANAG 1008 are proved insufficient to satisfy the respective variations.
- The effect of the upper bound of generator's field voltage is less significant and it only appears for values smaller than 2 (which are not usual).

The above analysis has proved that voltage/frequency limits proposed in STANAG 1008 can lead to different pulsed load power factor – pulsed load apparent power limitation curves depending on various parameters. Some of the most important affecting parameters are: the periodicity and the duty cycle of the pulsed load, the sub-transient reactance of the generators, their associated automatic voltage regulator (AVR) gain, the loading factor of the generator at the time of the pulsed load occurrence, the service load power factor, the equivalent length of the cable between the pulsed load with the generator, the ratio of the service load which is supplied by the same sub-network of the ship to the total one, etc. Therefore, the limitation curves proposed in STANAG 1008 are proved insufficient in many cases according to the above analysis. Under these circumstances, it seems necessary to redesign the respective constraints of STANAG 1008 taking into consideration the aforementioned parameters. A family of limitation curves or analytical mathematical expressions for pulsed load limit calculations invoking the examined parameters, if it is possible, will greatly enhance the design process.

REFERENCES

1. J. Prousalidis, E. Styvaktakis, I.K. Hatzilau, F.D. Kanellos, S. Perros and E. Sofras: "Electric Power Supply Quality in ship systems an overview", *International Journal of Ocean Systems Management*, Vol. 1, no.1 pp. 68 – 83 , 2008.
2. F.D. Kanellos, I.K. Hatzilau, J. Prousalidis, "Investigation of voltage/frequency modulation in ship electric networks with pulsed loads according to STANAG 1008 design constraints", All Electric Ship Conference 2007, London.

3. I.K. Hatzilau, J. Prousalidis, E. Styvaktakis, F.D. Kanellos, S. Perros, E. Sofras, "Electric Power Supply Quality Concepts for the All Electric Ship (AES)", World Maritime Technology Conference (WMTC2006), INEC 2006, IMarEST, 6-10 March 2006, London .
4. Howard A., Smolleck Satish J., Ranade Nadipuram R., Prasad Rudolph, O. Velasco, "Effects of Pulsed – Power Loads upon an Electric Power Grid", IEEE/PSS 1990 Sumner meeting, Minneapolis, Minnesota, July 15-19, 1990.
5. Z.W. Vilar, R.A. Dougal, "Effectiveness of generator control strategies on meeting pulsed load requirements in ship electric systems", IEEE ESTS 2005, July 25-27, 2005, Philadelphia, PA, USA
6. S.D. Sudhoff, B.T. Kuhn, E. Zivi, D.E. Delisle, D. Clayton, "Impact of Pulsed Power Loads on Naval Power and Propulsion Systems", 13th SCSS 2003, April 7-9, 2003, Orlando-Florida, USA
7. IEEE Std 45-1998, "IEEE Recommended Practice for Electrical Installations on Shipboard".
8. STANAG 1008, "Characteristics of Shipboard Electrical Power Systems in Warships of the NATO Navies", NATO, Edition 9, 24 Aug. 2004.
9. USA MIL-STD-1399(NAVY), "Interface standard for Shipboard systems – Section 300A – Electric Power, Alternating Current".
10. F.D. Kanellos, I.K. Hatzilau, J. Prousalidis, E. Styvaktakis,, "Simulation of a Shipboard Electrical Network (AES) comprising Pulsed Loads", Engine as a Weapon II, IMarEST, Dec. 2006, London.
11. P. Krause, "Analysis of Electric Machinery", McGraw-Hill, 1986.
12. Chee Chee-Mun Ong, "Dynamic Simulation of Electric Machinery using Matlab/Simulink", Prentice Hall PTR, 1998.